High Order Finite Difference Methods, Multidimensional Linear Problems and Curvilinear Coordinates

Jan Nordström
The Aeronautical Research Institute of Sweden, Bromma, Sweden

Mark H. Carpenter
NASA Langley Research Center, Hampton, Virginia

December 1999

The NASA STI Program Office . . . in Profile

Since its founding, NASA has been dedicated to the advancement of aeronautics and space science. The NASA Scientific and Technical Information (STI) Program Office plays a key part in helping NASA maintain this important role.

The NASA STI Program Office is operated by Langley Research Center, the lead center for NASA's scientific and technical information. The NASA STI Program Office provides access to the NASA STI Database, the largest collection of aeronautical and space science STI in the world. The Program Office is also NASA's institutional mechanism for disseminating the results of its research and development activities. These results are published by NASA in the NASA STI Report Series, which includes the following report types:
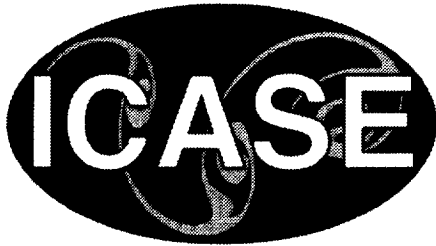
- TECHNICAL PUBLICATION. Reports of completed research or a major significant phase of research that present the results of NASA programs and include extensive data or theoretical analysis. Includes compilations of significant scientific and technical data and information deemed to be of continuing reference value. NASA counter-part or peer-reviewed formal professional papers, but having less stringent limitations on manuscript length and extent of graphic presentations.

- TECHNICAL MEMORANDUM. Scientific and technical findings that are preliminary or of specialized interest, e.g., quick release reports, working papers, and bibliographies that contain minimal annotation. Does not contain extensive analysis.

- CONTRACTOR REPORT. Scientific and technical findings by NASA-sponsored contractors and grantees.

- CONFERENCE PUBLICATIONS. Collected papers from scientific and technical conferences, symposia, seminars, or other meetings sponsored or co-sponsored by NASA.

- SPECIAL PUBLICATION. Scientific, technical, or historical information from NASA programs, projects, and missions, often concerned with subjects having substantial public interest.

- TECHNICAL TRANSLATION. English-language translations of foreign scientific and technical material pertinent to NASA's mission.

Specialized services that help round out the STI Program Office's diverse offerings include creating custom thesauri, building customized databases, organizing and publishing research results . . . even providing videos.

For more information about the NASA STI Program Office, you can:

- Access the NASA STI Program Home Page at http://www.sti.nasa.gov/STI-homepage.html

- Email your question via the Internet to help@sti.nasa.gov

- Fax your question to the NASA Access Help Desk at (301) 621-0134

- Phone the NASA Access Help Desk at (301) 621-0390

- Write to:
  NASA Access Help Desk
  NASA Center for AeroSpace Information
  7121 Standard Drive
  Hanover, MD 21076-1320

High Order Finite Difference Methods, Multidimensional Linear Problems and Curvilinear Coordinates

Jan Nordström
The Aeronautical Research Institute of Sweden, Bromma, Sweden

Mark H. Carpenter
NASA Langley Research Center, Hampton, Virginia

HIGH ORDER FINITE DIFFERENCE METHODS, MULTIDIMENSIONAL LINEAR PROBLEMS AND CURVILINEAR COORDINATES

JAN NORDSTRÖM* AND MARK H. CARPENTER†

Abstract. Boundary and interface conditions are derived for high order finite difference methods applied to multidimensional linear problems in curvilinear coordinates. The boundary and interface conditions lead to conservative schemes and strict and strong stability provided that certain metric conditions are met.

Key words. high-order finite-difference, numerical stability, interface conditions, summation-by-parts, variable coefficient

Subject classification. Applied and Numerical Mathematics

1. Introduction. Phenomena that require an accurate description of high frequency variation in space for long times occur in many important applications such as electromagnetics, acoustics (all cases of wave propagation), and direct simulation of turbulent and transitional flow; see for example [1]-[6]. Strictly stable high order finite difference methods are well suited for these types of problems (see [7]-[16]) because they guarantee accurate results with bounded error growth in time for realistic meshes.

Most of the development for these types of methods has considered constant coefficient problems on a Cartesian mesh. In [17], [18] stable and conservative boundary and interface conditions were derived for the one-dimensional constant coefficient Euler and Navier-Stokes equations on multiple domains. A similar technique was used in [19], [20], and [21] for Chebyshev spectral methods.

In this paper we extend the constant coefficient analysis in [17], [18] to scalar multidimensional linear problems in curvilinear coordinates including block interfaces. Related previous work includes investigations of the metric derivatives in non-smooth meshes (see [22], [23]) and the treatment of parabolic and hyperbolic systems in curvilinear coordinates on a single domain [14].

The rest of this paper will proceed as follows. Section 2, will give some basic definitions. Section 3 presents the 1D difference operators that form the basis of the multidimensional approximation treatment. Section 4 defines the linear model problem and discusses well-posedness. Section 5 provides an investigation of the discrete problem. Section 6 illustrates numerical experiments and in Section 7 we summarize and draw conclusions.

2. Definitions. Consider the linear initial boundary value problem

$$\begin{aligned}
w_t &= P(x,t)w + \delta F(x,t) &&, x \in \Omega \quad, t \geq 0, \\
w &= \delta f(x) &&, x \in \Omega \quad, t = 0, \\
L_c w &= \delta g(t) &&, x \in \Gamma \quad, t \geq 0,
\end{aligned}$$

(2.1)

where P is the differential operator, L_c is the boundary operator, Ω is the domain and Γ is the domain boundary. The forcing function δF, the initial function δf, and the boundary data δg are the data of the

problem; w denotes the difference between a solution with data f, F, g and one with data $f + \delta f$, $F + \delta F$, $g + \delta g$.

The semi-discrete version of (2.1) is

(2.2)
$$
\begin{aligned}
(w_j)_t &= Q(x_j, t)w_j + \delta F_j(t) &, x_j \in \Omega \quad, t \geq 0, \\
w_j &= \delta f_j &, x_j \in \Omega \quad, t = 0, \\
L_D w_j &= \delta g(t) &, x_j \in \Gamma \quad, t \geq 0,
\end{aligned}
$$

where Q is the difference operator approximating the differential operator P, δF_j is the forcing function, δf_j the initial function, L_D the discrete boundary operator where numerical boundary conditions are included, and δg the boundary data. It is assumed that (2.2) is a consistent approximation of (2.1).

2.1. Well-posedness and stability. There are many concepts of well-posedness and stability; see [24]. Here we consider the following definitions.

DEFINITION 1. *Problem (2.1) is strongly well posed if the solution w is unique, exists, and satisfies*

(2.3)
$$
\|w\|_\Omega^2 + \int_0^t \|w\|_\Gamma^2 dt \leq K_c e^{\eta_c t}\{\|\delta f\|_\Omega^2 + \int_0^t (\|\delta F\|_\Omega^2 + \|\delta g\|_\Gamma^2)dt\},
$$

where K_c and η_c may not depend on δF, δf, δg, and $\| \cdot \|_\Omega$ and $\| \cdot \|_\Gamma$ are suitable continuous norms.

DEFINITION 2. *Problem (2.2) is strongly stable if for a sufficiently fine mesh the solution w_j satisfies*

(2.4)
$$
\|w\|_\Omega^2 + \int_0^t \|w\|_\Gamma^2 dt \leq K_d e^{\eta_d t}\{\|\delta f\|_\Omega^2 + \int_0^t (\|\delta F\|_\Omega^2 + \|\delta g\|_\Gamma^2)dt\},
$$

where K_d and η_d may not depend on δF_j, δf_j, δg, and $\| \cdot \|_\Omega$ and $\| \cdot \|_\Gamma$ are suitable discrete norms.

DEFINITION 3. *The approximation (2.2) of (2.1) is strictly stable if the analytical and discrete growth rates (see (2.3) and (2.4)) satisfy*

(2.5)
$$
\eta_d \leq \eta_c + \mathcal{O}(\Delta x),
$$

where Δx is the mesh size.

2.2. Linear algebra relations. For later reference we define some useful matrix operations; see [25].

DEFINITION 4. *Let A be a $p \times q$ matrix, and B be an $m \times n$ matrix; then*

$$
A \odot B = \begin{pmatrix} a_{0,0}B & \cdots & a_{0,q-1}B \\ \vdots & & \vdots \\ a_{p-1,0}B & \cdots & a_{p-1,q-1}B \end{pmatrix}.
$$

The $p \times q$ block matrix $A \odot B$ is called a Kronecker product. There are a number of rules for Kronecker products; see [25]. In this paper we will make frequent use of

(2.6)
$$
\begin{aligned}
(A \odot B)(C \odot D) &= (AC) \odot (BD), \\
(A \odot B)^T &= A^T \odot B^T, \\
(A \odot B)^{-1} &= A^{-1} \odot B^{-1}.
\end{aligned}
$$

Consider the following matrices,

(2.7)
$$
B = B^T > 0, \quad C = C^T > 0, \quad D = diag(d_i) > 0,
$$

where B, C, and $B \odot C$ have the structure

$$(2.8) \qquad B = \begin{bmatrix} B^L & & & \\ & 1 & & \mathbf{0} \\ & & \ddots & \\ \mathbf{0} & & & 1 \\ & & & & B^R \end{bmatrix}, C = \begin{bmatrix} C^L & & & \\ & 1 & & \mathbf{0} \\ & & \ddots & \\ \mathbf{0} & & & 1 \\ & & & & C^R \end{bmatrix}.$$

We will need the following lemmas.

LEMMA 1. *Let C and D be the $M \times M$ matrices defined in (2.7)-(2.8). If the blocks C_L, C_R have dimension $r \times r$ and the first and last r components in D are constant, then*

$$(2.9) \qquad CD = DC = C^{1/2}DC^{1/2} > 0.$$

Proof: A direct matrix multiplication leads to (2.9). $\square$

LEMMA 2. *Let the first and last r components $D_k = diag(d_i), k = 1, ..., N$ be constants; let B have $q \times q$ blocks B_L, B_R and C have $r \times r$ blocks C_L, C_R; see (2.7)-(2.8). With $A = B \odot C$ and $D = diag(D_k)$ we have*

$$(2.10) \qquad AD = DA = A^{1/2}DA^{1/2} > 0$$

if the first $(D_1, ..., D_q)$ and last $(D_{N-(q-1)}, ..., D_N)$ q-blocks in D are equal. *Proof:* By introducing $D_L = (I_q \odot D_1)$ with I the identity matrix, the relations (2.6) and lemma 1, the upper left corner of AD becomes

$$(B_L \odot C)D_L = B_L \odot CD_1 = B_L \odot D_1 C = D_L(B_L \odot C)$$

and

$$(B_L \odot C)D_L = (B_L^{1/2} \odot C^{1/2})(B_L^{1/2} \odot D_1 C^{1/2}) = (B_L^{1/2} \odot C^{1/2})D_L(B_L^{1/2} \odot C^{1/2}).$$

Positive definiteness follows directly from the fact that $D_L > 0$. $\square$

3. The 1D difference operators. The 1D difference operators that form the basis for the multidimensional difference approximations will be presented below, for more information see [17], [18].

3.1. The discrete differentiation operator. Let U, $\mathcal{D}U$ be the numerical approximations of the scalar quantities u and u_x respectively. The approximation $\mathcal{D}U$ of the first derivative

$$(3.1) \qquad \mathcal{D}U = P^{-1}QU, \quad u_x - P^{-1}Qu = T_\epsilon, \quad |T_\epsilon| = \mathcal{O}(\Delta x^m, \Delta x^n)$$

where $|T_\epsilon| = \mathcal{O}(\Delta x^m, \Delta x^n)$ means that the approximation of the differential operator is accurate to order m in the interior of the domain and to order n at the boundary. Typically we have $n = m - 1$. The summation-by-parts (SBP) operator $\mathcal{D}U$ satisfies

$$(3.2) \qquad (U, \mathcal{D}V)_P = U_N V_N - U_0 V_0 - (\mathcal{D}U, V)_P$$

where

$$(3.3) \qquad (U, V)_P = U^T PV, \quad P = P^T, \quad Q + Q^T = D, \quad D = diag[-1, 0, ..., 0, 1]$$

and $0 < p_{min}\Delta x I \leq P \leq p_{max}\Delta x I$. Operators of the SBP type arise naturally with centered difference approximations; for examples see [9], [15], [12], [26].

In this paper we will apply the first derivative operator twice to obtain the second derivative; i.e., we will use

$$(3.4) \qquad \mathcal{D}^2 U = \mathcal{D}(\mathcal{D}U), \quad u_{xx} - P^{-1}QP^{-1}Qu = T_e, \quad T_e = \mathcal{O}(\Delta x^m, \Delta x^p)$$

despite the fact that we lose two orders of magnitude in accuracy $p = m - 2$ at the boundaries. The second derivative defined in (3.4) satisfies (3.2) with $V = B\mathcal{D}U$, which is completely similar to $(u, (bu_x)_x) = ubu_x|_0^1 - (u_x, bu_x)$ obtained in the continuous case. For another type of second derivative, see [17], [18].

3.2. The discrete integration operator. The matrix P in the SBP derivative operator is a discrete integration operator.

THEOREM 1. *Let the difference operator $\mathcal{D} = P^{-1}Q$ defined in (3.1)-(3.3) exists on the interval $-1 \le x \le 1$. Then, the matrix P is an integration operator which satisfies*

$$(3.5) \qquad \int_{-1}^{1} (uv)_x dx = U^T P \mathcal{D} V + (\mathcal{D}U)^T P V$$

where U, V are the projections of the continuous functions u, v onto the grid. Proof: $U^T P \mathcal{D} V + (\mathcal{D}U)^T PV = (UV)|_0^N = (uv)|_{-1}^{+1} = \int_{-1}^{1}(uv)_x dx.$ $\square$

It is also possible to prove the following theorem.

THEOREM 2. *Let the difference operator $P^{-1}Q$ defined in (3.1)-(3.3) exist on the interval $-1 \le x \le 1$ and be accurate to order m. Then, the matrix P is an integration operator which satisfies*

$$(3.6) \qquad \int_{-1}^{1} uv \ dx = U^T P V + \mathcal{O}(\Delta x^m).$$

where U, V are the projections of the continuous functions u, v onto the grid. Sketch of Proof: The proof has two parts. The first part shows that (3.6) holds for general polynomials. Next, Weistrass' interpolation theorem (see [28]) is used to show that it also holds for continuous functions.

4. The continuous problem. The definition and specification of the continuous problem is done with Cartesian coordinates. After the transformation to curvilinear coordinates we check that the essential mathematical properties are preserved.

4.1. Cartesian coordinates. The two-dimensional (2D) linear problem considered in this paper is

$$(4.1) \qquad \begin{aligned} u_t + F_x + G_y &= h, & [x,y] \in \Omega, & \quad t \ge 0 \\ u &= f, & [x,y] \in \Omega, & \quad t = 0 \\ Lu &= g, & [x,y] \in \delta\Omega, & \quad t \ge 0, \end{aligned}$$

where h, f, g are the data of the problem, L is the boundary operator, and

$$(4.2) \qquad \begin{aligned} F &= F^I + F^V, & F^I = a_1 u, & F^V = -(b_{11}u_x + b_{12}u_y), \\ G &= G^I + G^V, & G^I = a_2 u, & G^V = -(b_{21}u_x + b_{22}u_y). \end{aligned}$$

The coefficients a_i, b_{ij} are known functions of x, y, and t. For simplicity we have chosen $\Omega = [x,y] \in [-1,1] \times [0,1]$; see figure 4.1. For future reference we also introduce

$$(4.3) \qquad \vec{a} = (a_1, a_2), \quad \vec{F} = (F, G), \quad \vec{n} = (n_1, n_2),$$

where $\vec{n}$ is the outward pointing unit normal on $\delta\Omega$.

Equation (4.1) can be thought of as a model for the Euler, Navier-Stokes, or Maxwell's equations.
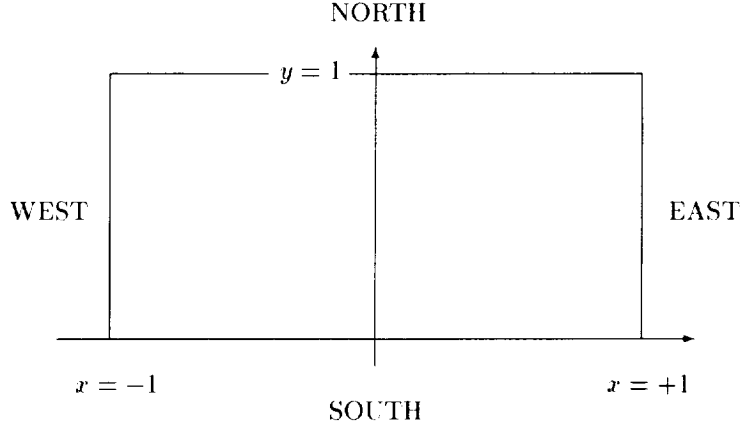
FIG. 4.1. *The computational domain.*

4.1.1. The energy estimate. Well-posedness of (4.1) requires that we can obtain an energy estimate. Let

$$(4.4) \qquad (u,v) = \int_0^1 \int_{-1}^1 uv \ dxdy, \quad (u,u) = \|u\|^2,$$

$$(4.5) \qquad (u,v)_{E,W} = \int_0^1 (uv)_{E,W} dy, \quad (u,u)_{E,W} = \|u\|^2_{E,W}$$

$$(4.6) \qquad (u,v)_{N,S} = \int_{-1}^1 (uv)_{N,S} dx, \quad \|u\|^2_{N,S} = (u,u)_{N,S}\|u\|^2_{N,S} = (u,u)_{N,S}$$

denote the L_2 scalar product, the L_2 norm, the boundary scalar products, and the boundary norms respectively. The subscripts E,W,N,S refer to the EAST, WEST, NORTH, and SOUTH boundaries (see figure 4.1).

The energy method applied to (4.1) leads to

$$\|u\|^2_t = -\underbrace{[(u,F^I + 2F^V)_E - (u,F^I + 2F^V)_W]}_{\text{EAST-WEST}}$$

$$-\underbrace{[(u,G^I + 2G^V)_N - (u,G^I + 2G^V)_S]}_{\text{NORTH-SOUTH}}$$

$$-\underbrace{[(u,F_x^I) - (u_x,F^I) + (u,G_y^I) - (u_y,G^I)]}_{\text{GROWTH 1}} + \underbrace{[(u,h) + (h,u)]}_{\text{GROWTH 2}}$$

$$(4.7) \qquad -\underbrace{[(u_x,F^V) + (F^V,u_x) + (u_y,G^V) + (G^V,u_y)]}_{\text{DISSIPATION}}.$$

GROWTH 1 (GR1) and GROWTH 2 (GR2) in (4.7) will lead to a growth or decay in $\|u\|^2$, but will not affect well-posedness. Note that for constant coefficient problems GR1 is zero. To bound $\|u\|^2$ in time, the first two terms must be bounded using the correct boundary conditions and the DISSIPATION (DI) must have the right sign.

4.1.2. The dissipation. For a correct sign of DI (see (4.2) and (4.7)) the eigenvalues of $B + B^T$ where

$$(4.8) \qquad B = \begin{bmatrix} b_{11} & b_{12} \\ b_{21} & b_{22} \end{bmatrix}$$

must be positive; therefore,

$$(4.9) \qquad b_{11} > 0, \quad b_{22} > 0, \quad b_{11}b_{22} - \left(\frac{b_{12} + b_{21}}{2}\right)^2 > 0$$

is a requirement for well-posedness.

4.1.3. Boundary conditions. By integrating the "cross derivative" components of the first two terms in (4.7) one obtains

$$-\int_0^1 u(F^I + 2F^V)|_{-1}^{+1}dy - \int_{-1}^1 u(G^I + 2G^V)|_0^1 dx = (b_{12} + b_{21})u^2|_{-1}^{+1}|_0^1$$

$$-\int_0^1 u((a_1 + (b_{12})_y)u - 2b_{11}u_x)|_{-1}^{+1}dy - \int_{-1}^1 u((a_2 + (b_{21})_x)u - 2b_{22}u_y)|_0^1 dx.$$

The term $(b_{12} + b_{21})u^2|_{-1}^{+1}|_0^1$ involves the point values in the four corners of the computational domain. These point values cannot be estimated (unless they are artificially specified). Boundary conditions where the viscous fluxes (F^V, G^V) are specified avoid that difficulty and lead to an energy estimate; therefore one should specify the total flux $(F = F^I + F^V, G = G^I + G^V)$ or the viscous flux at the boundaries.

Consider the first two terms in (4.7) and recall the definition (4.3). At $x = \pm 1$ with $\vec{n} = (\pm 1, 0)$ we have the boundary conditions

$$(4.10) \qquad \begin{array}{rclcrclcrcl}
-a_1(-1, y, t) & = & \vec{a} \cdot \vec{n} \le 0 & \vec{F} \cdot \vec{n} & = & F & = & F_W(y, t), \\
-a_1(-1, y, t) & = & \vec{a} \cdot \vec{n} > 0 & \vec{F}^V \cdot \vec{n} & = & F^V & = & F_W^V(y, t), \\
+a_1(+1, y, t) & = & \vec{a} \cdot \vec{n} > 0 & \vec{F}^V \cdot \vec{n} & = & F^V & = & F_E^V(y, t), \\
+a_1(+1, y, t) & = & \vec{a} \cdot \vec{n} \le 0 & \vec{F} \cdot \vec{n} & = & F & = & F_E(y, t),
\end{array}$$

while

$$(4.11) \qquad \begin{array}{rclcrclcrcl}
-a_2(x, 0, t) & = & \vec{a} \cdot \vec{n} \le 0 & \vec{F} \cdot \vec{n} & = & G & = & G_S(x, t), \\
-a_2(x, 0, t) & = & \vec{a} \cdot \vec{n} > 0 & \vec{F}^V \cdot \vec{n} & = & G^V & = & G_S^V(x, t), \\
+a_2(x, 1, t) & = & \vec{a} \cdot \vec{n} > 0 & \vec{F}^V \cdot \vec{n} & = & G^V & = & G_N^V(x, t), \\
+a_2(x, 1, t) & = & \vec{a} \cdot \vec{n} \le 0 & \vec{F} \cdot \vec{n} & = & G & = & G_N(x, t),
\end{array}$$

are used at $y = 0, 1$ where $\vec{n} = (0, \mp 1)$. The boundary conditions (4.10), (4.11) can also be formulated in the following more general way.

$$(4.12) \qquad \begin{array}{rclcl}
\vec{a} \cdot \vec{n} \le 0 & \Rightarrow & \vec{F} \cdot \vec{n} & = & \vec{F}_{\delta\Omega} \cdot \vec{n} \\
\vec{a} \cdot \vec{n} > 0 & \Rightarrow & \vec{F}^V \cdot \vec{n} & = & \vec{F}_{\delta\Omega}^V \cdot \vec{n}
\end{array}$$

Boundary conditions of the type (4.10), (4.11), (4.12) have been derived in [29] and [20] for the Navier-Stokes equations.

Let us consider the EAST boundary in detail, and let us assume that a_1 is positive at $y = 0$, becomes negative at $y = y_0$ and remains negative until $y = 1$. Inserting the boundary conditions (4.10) into (4.7) yields

$$-\int_0^1 u(F^I + 2F^V)|_E dy = -\int_0^{y_0} |a_1(1, y, t)|u^2 + 2uF_E^V dy$$

$$+\int_{y_0}^1 a_1(1, y, t)u^2 - 2uF_E dy = -\int_0^{y_0} |a_1|u^2 + 2uF_E^V dy$$

$$(4.13) \qquad -\int_{y_0}^1 |a_1|u^2 + 2uF_E dy = -\int_0^1 |a_1|u^2 + 2u(\sigma_1 F_E^I + F_E^V)dy,$$

where $\sigma_1 = (1 - |a_1|/a_1)/2$. The requirement that a_1 changes sign in the manner described above can be relaxed, so (4.13) is a generally valid formula. An entirely similar procedure at the other (WEST, NORTH, SOUTH) boundaries yields the final result:

$$-(u, F^I + 2F^V)_E = -(u, |a_1|u)_E - 2(u, \tilde{F}_E)_E,$$

$$(u, F^I + 2F^V)_W = -(u, |a_1|u)_W - 2(u, \tilde{F}_W)_W,$$

$$-(u, G^I + 2G^V)_N = -(u, |a_2|u)_N - 2(u, \tilde{G}_N)_N,$$

(4.14) $$(u, G^I + 2G^V)_S = -(u, |a_2|u)_S - 2(u, \tilde{G}_S)_S.$$

where

$$\tilde{F}_E = \sigma_1 F_E + (1 - \sigma_1)F_E^V, \quad \sigma_1 = (1 - |a_1|/a_1)/2,$$

$$\tilde{F}_W = \sigma_3 F_W + (1 - \sigma_3)F_W^V, \quad \sigma_3 = -(1 + |a_1|/a_1)/2,$$

$$\tilde{G}_N = \sigma_5 G_N + (1 - \sigma_5)G_N^V, \quad \sigma_5 = (1 - |a_2|/a_2)/2,$$

(4.15) $$\tilde{G}_S = \sigma_7 G_S + (1 - \sigma_7)G_S^V, \quad \sigma_7 = -(1 + |a_2|/a_2)/2.$$

Inserting the relations (4.14) and (4.15) into (4.7) leads to

(4.16) $$\|u\|_t^2 \le \sum_{I=E,W,N,S} \frac{1}{\eta_I}\|\tilde{F}_I\|_I^2 + \text{GR1} + \text{GR2} + \text{DI},$$

where

$$\eta_E = \frac{\int_0^1 |a_1|u^2 dy}{\int_0^1 u^2 dy}\Big|_{x=1}, \quad \eta_W = \frac{\int_0^1 |a_1|u^2 dy}{\int_0^1 u^2 dy}\Big|_{x=-1},$$

$$\eta_N = \frac{\int_{-1}^1 |a_2|u^2 dx}{\int_{-1}^1 u^2 dx}\Big|_{y=1}, \quad \eta_S = \frac{\int_{-1}^1 |a_2|u^2 dx}{\int_{-1}^1 u^2 dx}\Big|_{y=0}.$$

The parameters $\eta_E, \eta_W, \eta_N, \eta_S$ are strictly positive if a_1, a_2 are zero for a finite number of points.

Time-integration of (4.16) leads to an energy estimate of the form (2.3) if (4.9) holds. Provided that a solution exists (can be shown by using the Laplace-transform technique or via difference approximations; see [30] and [31]), we can conclude that the following theorem holds.

THEOREM 3. *Problem (4.1), (4.10), (4.11) is strongly well posed.*

4.2. Curvilinear coordinates. In this Section we consider problem (4.1) on a curvilinear domain. By introducing the transformation $t = \tau, x = x(\xi, \eta, \tau), y = y(\xi, \eta, \tau)$ and it's inverse

(4.17) $$\tau = t, \quad \xi = \xi(x, y, t), \quad \eta = \eta(x, y, t),$$

we obtain the transformed equation

(4.18) $$(Ju)_\tau + (J(\xi_t u + \xi_x F + \xi_y G))_\xi + (J(\eta_t u + \eta_x F + \eta_y G))_\eta = Jh + RHS,$$

where

$$RHS = u(J_t + (J\xi_t)_\xi + (J\eta_t)_\eta) + F((J\xi_x)_\xi + (J\eta_x)_\eta) + G((J\xi_y)_\xi + (J\eta_y)_\eta).$$

7

Using the metric relations causes the term RHS to vanish:

$$(4.19) \quad \begin{aligned} J\xi_t &= (x_\eta y_\tau - x_\tau y_\eta) & J\eta_t &= (y_\xi x_\tau - x_\xi y_\tau) \\ J\xi_x &= y_\eta & J\xi_y &= -x_\eta \\ J\eta_x &= -y_\xi & J\eta_y &= x_\xi \\ J &= x_\xi y_\eta - x_\eta y_\xi & J &= (\xi_x \eta_y - \xi_y \eta_x)^{-1}. \end{aligned}$$

In this paper we will consider the steady version of (4.17), i.e., $\xi = \xi(x,y), \eta = \eta(x,y)$. The new transformed problem becomes

$$(4.20) \quad \begin{aligned} Ju_\tau + (F)_\xi + (G)_\eta &= h, & [\xi,\eta] \in \Omega, & \quad \tau \geq 0, \\ u &= f, & [\xi,\eta] \in \Omega, & \quad \tau = 0, \\ Lu &= g, & [\xi,\eta] \in \delta\Omega, & \quad \tau \geq 0, \end{aligned}$$

where $h = Jh, f, g$ are the data of the problem and $\Omega = [\xi,\eta] \in [-1,1] \times [0,1]$. The new transformed fluxes are

$$(4.21) \quad \begin{aligned} F &= J(\vec{F} \cdot \nabla \xi) = F^I + F^V, & F^I &= a_1 u, & F^V &= -[b_{11} u_\xi + b_{12} u_\eta], \\ G &= J(\vec{F} \cdot \nabla \eta) = G^I + G^V, & G^I &= a_2 u, & G^V &= -[b_{21} u_\xi + b_{22} u_\eta], \end{aligned}$$

where

$$(4.22) \quad \begin{aligned} a_1 &= J\vec{a} \cdot \nabla \xi & b_{11} &= J\nabla\xi \cdot B\nabla\xi & b_{12} &= J\nabla\xi \cdot B\nabla\eta \\ a_2 &= J\vec{a} \cdot \nabla\eta & b_{21} &= J\nabla\eta \cdot B\nabla\xi & b_{22} &= J\nabla\eta \cdot B\nabla\eta \end{aligned}$$

and B is given in (4.8).

4.2.1. The energy method. Let

$$(4.23) \quad (u,v)_J = \int_0^1 \int_{-1}^1 (uv) \quad Jd\xi d\eta, \quad \|u\|_J^2 = (u,u)_J,$$

$$(4.24) \quad (u,v) = \int_0^1 \int_{-1}^1 (uv) \quad d\xi d\eta, \quad \|u\|^2 = (u,u),$$

$$(4.25) \quad (u,v)_{E,W} = \int_0^1 (uv)_{E,W} \quad d\eta, \quad \|u\|_{E,W}^2 = (u,u)_{E,W},$$

$$(4.26) \quad (u,v)_{N,S} = \int_{-1}^1 (uv)_{N,S} \quad d\xi, \quad \|u\|_{N,S}^2 = (u,u)_{N,S}$$

denote the weighted L_2 scalar product and norm, the L_2 scalar product and norm, the boundary scalar products, and boundary norms respectively. The subscripts E, W, N, S refer to the EAST,WEST,NORTH and SOUTH boundaries as in figure 4.1, with x, y replaced by ξ, η.

The equation corresponding to (4.7) becomes,

$$(\|u\|_J^2)_\tau = - \underbrace{[(u,F^I + 2F^V)_E - (u,F^I + 2F^V)_W]}_{\text{EAST-WEST}}$$
$$- \underbrace{[(u,G^I + 2G^V)_N - (u,G^I + 2G^V)_S]}_{\text{NORTH-SOUTH}}$$

8

$$-\underbrace{[(u,F_\xi^I)-(u_\xi,F^I)+(u,G_\eta^I)-(u_\eta,G^I)]}_{\text{GROWTH 1}}+\underbrace{[(u,h)+(h,u)]}_{\text{GROWTH 2}}$$

(4.27)
$$-\underbrace{[(u_\xi,F^V)+(F^V,u_\xi)+(u_\eta,G^V)+(G^V,u_\eta)]}_{\text{DISSIPATION}}.$$

Precisely as in the Cartesian case, GR1 and GR2 in (4.27) can lead to a growth or decay in $\|u\|_J^2$, but will not affect well-posedness. The metric relations (4.19) show that in the curvilinear case too, GR1 vanishes for constant coefficient problems. Just as in the Cartesian case, we need to assure that DI has the right sign.

4.2.2. The dissipation. Similar conditions as in the Cartesian case for positive eigenvalues also apply in the curvilinear case; see (4.27). Thus we must show that

(4.28)
$$b_{11}>0, \quad b_{22}>0, \quad b_{11}b_{22}-\left(\frac{b_{12}+b_{21}}{2}\right)^2>0$$

to assure the right sign on DI. The conditions (4.28) hold, since (4.22), (4.8), and (4.9) lead to $2b_{11}=J\nabla\xi^T(B+B^T)\nabla\xi>0, 2b_{22}=J\nabla\eta^T(B+B^T)\nabla\eta>0$, and

$$b_{11}b_{22}-\left(\frac{b_{12}+b_{21}}{2}\right)^2=b_{11}b_{22}-\left(\frac{b_{12}+b_{21}}{2}\right)^2>0.$$

4.2.3. Boundary conditions. Consider the first two terms in (4.27) and recall the definitions (4.3). The outward pointing unit normal on $\delta\Omega$ is,

(4.29)
$$\vec{n}(\xi=\pm1,\eta)=\frac{\pm\nabla\xi}{|\nabla\xi|}, \quad \vec{n}(\xi,\eta=0,1)=\frac{\mp\nabla\eta}{|\nabla\eta|},$$

where $|\nabla\xi|=\sqrt{\xi_x^2+\xi_y^2}$ and $|\nabla\eta|=\sqrt{\eta_x^2+\eta_y^2}$. The boundary conditions leading to an energy estimate become

(4.30)
$$\begin{array}{rclclcl}
-a_1(-1,\eta,t) &=& -J\vec{a}\cdot\nabla\xi\le0 & J\vec{F}\cdot\nabla\xi &=& F &=& F_W(\eta,t),\\
-a_1(-1,\eta,t) &=& -J\vec{a}\cdot\nabla\xi>0 & J\vec{F}^V\cdot\nabla\xi &=& F^V &=& F_W^V(\eta,t),\\
+a_1(+1,\eta,t) &=& J\vec{a}\cdot\nabla\xi>0 & J\vec{F}^V\cdot\nabla\xi &=& F^V &=& F_E^V(\eta,t),\\
+a_1(+1,\eta,t) &=& J\vec{a}\cdot\nabla\xi\le0 & J\vec{F}\cdot\nabla\xi &=& F &=& F_E(\eta,t)
\end{array}$$

at $\xi=\pm1$, while

(4.31)
$$\begin{array}{rclclcl}
-a_2(\xi,0,t) &=& -J\vec{a}\cdot\nabla\eta\le0 & J\vec{F}\cdot\nabla\eta &=& G &=& G_S(\xi,t),\\
-a_2(\xi,0,t) &=& -J\vec{a}\cdot\nabla\eta>0 & J\vec{F}^V\cdot\nabla\eta &=& G^V &=& G_S^V(\xi,t),\\
+a_2(\xi,1,t) &=& J\vec{a}\cdot\nabla\eta>0 & J\vec{F}^V\cdot\nabla\eta &=& G^V &=& G_N^V(\xi,t),\\
+a_2(\xi,1,t) &=& J\vec{a}\cdot\nabla\eta\le0 & J\vec{F}\cdot\nabla\eta &=& G &=& G_N(\xi,t)
\end{array}$$

should be used at $\eta=0,1$. The boundary conditions (4.30), (4.31) can also be formulated as in (4.12).

The same procedure as in the Cartesian case leads to the estimate

(4.32)
$$(\|u\|_J^2)_\tau\le\sum_{I=E,W,N,S}\frac{1}{\eta_I}\|\tilde{F}_I\|_I^2+\text{GR1}+\text{GR2}+\text{DI},$$

where

$$\tilde{F}_E=\sigma_1F_E+(1-\sigma_1)F_E^V, \quad \sigma_1=\frac{1}{2}(1-|a_1|/a_1).$$

$$\tilde{F}_W = \sigma_3 F_W + (1 - \sigma_3)\hat{F}_W^V, \quad \sigma_3 = -\frac{1}{2}(1 + |a_1|/a_1),$$

$$\tilde{G}_N = \sigma_5 G_N + (1 - \sigma_5)\hat{G}_N^V, \quad \sigma_5 = \frac{1}{2}(1 - |\dot{a}_2|/\dot{a}_2),$$

(4.33)
$$\tilde{G}_S = \sigma_7 \dot{G}_S + (1 - \sigma_7)\dot{G}_S^V, \quad \sigma_7 = -\frac{1}{2}(1 + |a_2|/a_2),$$

and

$$\eta_E = \frac{\int_0^1 |\dot{a}_1| u^2 d\eta}{\int_0^1 u^2 d\eta}\Big|_{\xi=1}, \quad \eta_W = \frac{\int_0^1 |a_1| u^2 d\eta}{\int_0^1 u^2 d\eta}\Big|_{\xi=-1},$$

$$\eta_N = \frac{\int_{-1}^1 |\dot{a}_2| u^2 d\xi}{\int_{-1}^1 u^2 d\xi}\Big|_{\eta=1}, \quad \eta_S = \frac{\int_{-1}^1 |a_2| u^2 d\xi}{\int_{-1}^1 u^2 d\xi}\Big|_{\eta=0}.$$

The parameters $\eta_E, \eta_W, \eta_N, \eta_S$ are strictly positive if $a_1, \dot{a}_2$ are zero for a finite number of points.

Time-integration of the estimate (4.32) leads to an energy estimate of the form (2.3) if (4.28) holds. Provided that a solution exists we can conclude that the following theorem holds.

THEOREM 4. *Problem (4.20), (4.30), (4.31) is strongly well posed.*

4.3. Interface conditions. Boundary and interface conditions of the flux type (see (4.10), (4.11), (4.30), and (4.31)) require extra careful treatment; see [27] for an example.

4.3.1. Interface conditions in the curvilinear case. To apply the SAT technique [16] on the fluxes at an interface between two blocks with different coordinate transformations and matching gridlines (see [17], [18] for the one-dimensional treatment) requires that we identify the continuous part. Matching gridlines at $\xi = \xi_0 = const$ implies

(4.34)
$$(x_\xi)_1 \neq (x_\xi)_2, \quad (y_\xi)_1 \neq (y_\xi)_2, \quad (x_\eta)_1 = (x_\eta)_2, \quad (y_\eta)_1 = (y_\eta)_2$$

while we have

(4.35)
$$(x_\xi)_1 = (x_\xi)_2, \quad (y_\xi)_1 = (y_\xi)_2, \quad (x_\eta)_1 \neq (x_\eta)_2, \quad (y_\eta)_1 \neq (y_\eta)_2$$

at $\eta = \eta_0 = const$. The subscripts $1, 2$ refer to the two coordinate transformations.

Equations (4.21), (4.19), and (4.34), (4.35) immediately lead to the conclusion that

(4.36)
$$F_1(\xi_0, \eta, \tau) = F_2(\xi_0, \eta, \tau), \quad G_1(\xi_0, \eta, \tau) \neq G_2(\xi_0, \eta, \tau),$$

(4.37)
$$F_1(\xi, \eta_0, \tau) \neq F_2(\xi, \eta_0, \tau), \quad G_1(\xi, \eta_0, \tau) = G_2(\xi, \eta_0, \tau);$$

i.e., F is continuous across $\xi = const$ while G is continuous across $\eta = const$.

4.3.2. Interface conditions and vanishing wave speeds. Another problem with flux-interface conditions appears when the wave speed a goes to zero. Consider the two constant coefficient problems

$$u_t + F(u)_x = 0, \quad -L \leq x \leq 0 \quad \text{and} \quad v_t + F(v)_x = 0, \quad 0 \leq x \leq L,$$

where $F(w) = aw + F^V(w)$, $F^V(w) = -\epsilon w_x$. Both problems have homogeneous outer boundary conditions at $|x| = L$ and zero initial data, and they are connected through interface conditions at $x = 0$. We

will compare the effects of flux-interface conditions $(F(u) = F(v), F^V(u) = F^V(v))$ and variable-interface conditions $(u = v, u_x = v_x)$ on the solutions.

By transforming the problem for v on $[0, +L]$ onto $[-L, 0]$ via the transformation $x \to -\xi$, and then replacing ξ with x, we obtain

$$
\begin{aligned}
\psi_t + \Lambda \psi_x &= \epsilon \psi_{xx}, & t &\geq 0, & -L &\leq x \leq 0, \\
\psi &= 0, & t &= 0, & -L &\leq x \leq 0, \\
B_{-L} \psi &= 0, & t &\geq 0, & x &= -L, \\
B_0 \psi &= 0, & t &\geq 0, & x &= 0,
\end{aligned}
$$

(4.38)

where $\psi = (u, v)^T$, $\Lambda = diag(a, -a)$, and $B_{-L} \psi = 0$ denotes the outer boundary conditions. $B_0 \psi = 0$ represents the transformed interface conditions

(4.39) $\qquad au - \epsilon u_x = av + \epsilon v_x, \quad -\epsilon u_x = +\epsilon v_x \quad \text{or} \quad u = v, \quad u_x = -v_x.$

We will treat (4.38) as a half-plane problem, which means that we let $L \to \infty$ and replace the influence of B_{-L} by only admitting bounded solutions as $x \to -\infty$.

The Laplace-transform technique applied to (4.38) leads to

$$\tilde{u}(x, s) = \sigma_1(s) \exp(\kappa_1(s)x), \quad \tilde{v}(x, s) = \sigma_2(s) \exp(\kappa_2(s)x)$$

where s is the dual variable with respect to time and

$$\kappa_1 = +\frac{a}{2\epsilon} + \sqrt{(\frac{a}{2\epsilon})^2 + \frac{s}{\epsilon}}, \quad \kappa_2 = -\frac{a}{2\epsilon} + \sqrt{(\frac{a}{2\epsilon})^2 + \frac{s}{\epsilon}}.$$

Note that both $\tilde{u}$, and $\tilde{v}$ decay away from the boundary $x = 0$.

The interface conditions (4.39) lead to the equation $E(s)\vec{\sigma} = 0$ where $\vec{\sigma} = (\sigma_1, \sigma_2)^T$. A well-posed bounded solution is obtained only if $det(E(s)) \neq 0$ for $\Re(s) > 0$. The flux-interface conditions in (4.39 lead to

(4.40) $\qquad E(s) = \begin{pmatrix} a - \epsilon\kappa_1 & -a - \epsilon\kappa_2 \\ -\epsilon\kappa_1 & -\epsilon\kappa_2 \end{pmatrix} \quad \Rightarrow \quad det(E(s)) = -2\epsilon a\sqrt{(\frac{a}{2\epsilon})^2 + \frac{s}{\epsilon}},$

while the variable-interface conditions leads to

(4.41) $\qquad E(s) = \begin{pmatrix} 1 & -1 \\ \kappa_1 & \kappa_2 \end{pmatrix} \quad \Rightarrow \quad det(E(s)) = 2\sqrt{(\frac{a}{2\epsilon})^2 + \frac{s}{\epsilon}}.$

Obviously the flux-interface conditions can lead to unbounded growth for vanishing wave speeds, because $det(E)_{a \to 0} = 0$ independent of s. The variable-interface conditions, on the other hand, lead to a well-posed problem since $det(E)_{a \to 0} = 2\sqrt{(s/\epsilon)}$.

A similar analysis of the flux-boundary condition $au - \epsilon u_x = 0$ for the single domain yields $det(E(s)) = a/2 + \sqrt{(a/2)^2 + s\epsilon}$. Consequently, the problem with unbounded growth for vanishing wave speed does not exist in the boundary condition case because $det(E)_{a \to 0} = \sqrt{(s\epsilon)}$.

5. The discrete problem on a curvilinear mesh. In the rest of this paper we will consider the transformed problem (4.20), (4.30), (4.31). Note that problem (4.1), (4.10),(4.11) corresponds to the special case where $\tau = t, \xi = x$ and $\eta = y$. For notational simplicity, we ignore the "hat" notation for the fluxes and transformed coefficients introduced in (4.20)-(4.22).
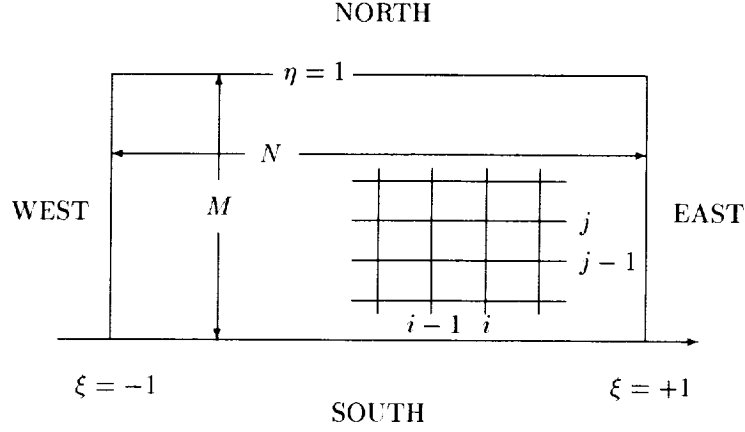
FIG. 5.1. *The single-domain case in transformed space.*

Let the $N \times N$ matrix P_ξ and the $M \times M$ matrix P_η be the 1D positive definite matrices defined in Section 3.1. A product av is arranged discretely (where $av \approx AV$) in the following way (see Figure 5.1):

$$(5.1) \qquad AV = \begin{bmatrix} \tilde{A}_1 & & & \\ & \tilde{A}_2 & & \mathbf{0} \\ & & \ddots & \\ \mathbf{0} & & \tilde{A}_{N-1} & \\ & & & \tilde{A}_N \end{bmatrix} \begin{bmatrix} \tilde{V}_1 \\ \tilde{V}_2 \\ \vdots \\ \vdots \\ \tilde{V}_{N-1} \\ \tilde{V}_N \end{bmatrix}, \quad \tilde{V}_i = \begin{bmatrix} V_{i1} \\ V_{i2} \\ \vdots \\ \vdots \\ V_{iM-1} \\ V_{iM} \end{bmatrix},$$

where $\tilde{A}_i = diag(a_{ij})$. Also, the $N \times N$ matrices J_E, J_W, I_ξ and the $M \times M$ matrices J_N, J_S, I_η are

$$(5.2) \qquad J_E = \begin{bmatrix} 0 & \cdots & 0 \\ \vdots & \ddots & \vdots \\ 0 & \cdots & 1 \end{bmatrix}, \quad J_W = \begin{bmatrix} 1 & \cdots & 0 \\ \vdots & \ddots & \vdots \\ 0 & \cdots & 0 \end{bmatrix}, \quad I_\xi = \begin{bmatrix} 1 & \cdots & 0 \\ \vdots & \ddots & \vdots \\ 0 & \cdots & 1 \end{bmatrix},$$

$$(5.3) \qquad J_N = \begin{bmatrix} 0 & \cdots & 0 \\ \vdots & \ddots & \vdots \\ 0 & \cdots & 1 \end{bmatrix}, \quad J_S = \begin{bmatrix} 1 & \cdots & 0 \\ \vdots & \ddots & \vdots \\ 0 & \cdots & 0 \end{bmatrix}, \quad I_\eta = \begin{bmatrix} 1 & \cdots & 0 \\ \vdots & \ddots & \vdots \\ 0 & \cdots & 1 \end{bmatrix},$$

respectively. The subscripts E, W, N, S refers to the EAST, WEST, NORTH, and SOUTH boundaries (see figure 5.1). At this point we also define the restriction of U to the boundaries:

$$(5.4) \qquad U_{E,W} = (J_{E,W} \odot I_\eta)U, \quad U_{N,S} = (I_\xi \odot J_{N,S})U.$$

5.1. The norms in the transformed problem. The norms and scalar-products corresponding to (4.23)-(4.26) are

$$(5.5) \qquad (U,V)_J = U^T(P_\xi \odot P_\eta)JV, \quad (U,U)_J = \|U\|_J^2,$$

$$(5.6) \qquad (U,V) = U^T(P_\xi \odot P_\eta)V, \quad (U,U) = \|U\|^2,$$

$$(5.7) \qquad (U,V)_{E,W} = U^T(J_{E,W} \odot P_\eta)V = U_{E,W}^T P_\eta V_{E,W}, \quad \|U\|_{E,W}^2 = (U,U)_{E,W},$$
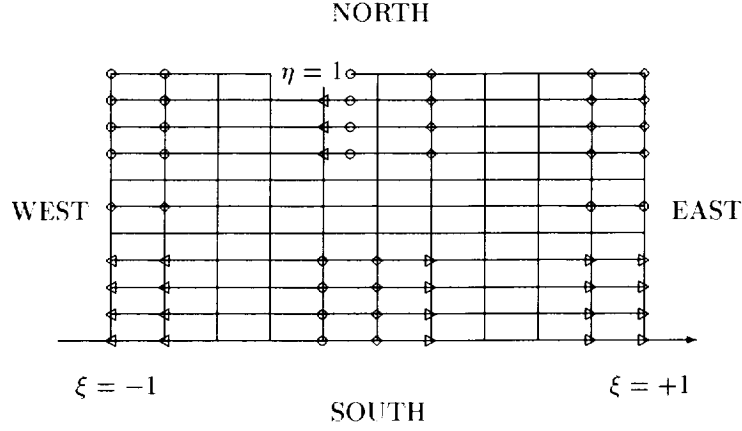
12

FIG. 5.2. *Schematic showing J requirements necessary for MJ to be a norm: $r = 4$ and $q = 2$.*

$$(5.8) \qquad (U,V)_{N,S} = U^T(P_\xi \odot J_{N,S})V = U_{N,S}^T P_\xi V_{N,S}, \quad \|U\|_{N,S}^2 = (U,U)_{N,S}.$$

Obviously, the relations (5.6)-(5.8) define norms since P_ξ and P_η are positive definite matrices. What about $(P_\xi \odot P_\eta)J$ in (5.5) ?

The metric scalar J is defined in (4.19). In matrix formulation we have

$$(5.9) \qquad J = diag(\tilde{J}_i), i = 1, ..., N \quad \tilde{J}_i = diag(J_{ij}), j = 1, ..., M.$$

We need the following theorem.

THEOREM 5. *Let $M = P_\xi \odot P_\eta$. If the first and last r components in $\tilde{J}_i$ are constants and the first $(\tilde{J}_1, ..., \tilde{J}_q)$ and last $(\tilde{J}_{N-(q-1)}, ..., \tilde{J}_N)$ q blocks in J are equal, then MJ is a norm.* Proof: Lemma 2, with $B = P_\xi, C = P_\eta$, and $D = J$, with J defined in (5.9), leads directly to $MJ = JM = M^{1/2}JM^{1/2} > 0$ $\square$.

The requirements in theorem 5 are illustrated in figure 5.2 (for $r = 4$ and $q = 2$) where $r \times q$ values of J are equal in the corners and r, q values of J are constant normal to an $\eta = const, \xi = const$ boundary respectively. A curvilinear transformation with such a J close to $\delta\Omega$ is called volume preserving and guarantees that MJ is a norm.

Remark. The conditions in theorem 5 (i.e., that J must be constant in the first q, r points normal and adjacent to the boundary $\delta\Omega$) can be thought of as theoretically ideal conditions. In practise one approaches the ideal condition with increasing resolution on a smooth mesh close to the boundary because

$$J(i,j) - J(0,j) = J_\xi(0,\eta_j)(i\Delta\xi) + \mathcal{O}(\Delta\xi^2), \quad i = 1, ..., q.$$

$$J(i,j) - J(i,0) = J_\eta(\xi_i,0)(j\Delta\eta) + \mathcal{O}(\Delta\eta^2), \quad j = 1, ..., r.$$

where it is assumed that $J(0,j), J(i,0)$ are the values of J at the boundaries. This process is illustrated in figure 5.3, where the minimum eigenvalue of $PD + DP$ as a function of increasing resolution is shown. The minimum eigenvalue goes from a negative value for large Δx to a positive one for small Δx.

5.2. The single-domain problem. The discrete formulation of (4.20), (4.30), (4.31) with the SAT technique [16] for incorporating flux boundary conditions is

$$(5.10) \qquad JU_\tau + D_\xi F + D_\eta G = h + BC, \quad U(0) = f.$$

where the continuous derivatives F_ξ, G_η are approximated with

$$(5.11) \qquad D_\xi F = (P_\xi^{-1}Q_\xi \odot I_\eta)F, \quad D_\eta G = (I_\xi \odot P_\eta^{-1}Q_\eta)G$$
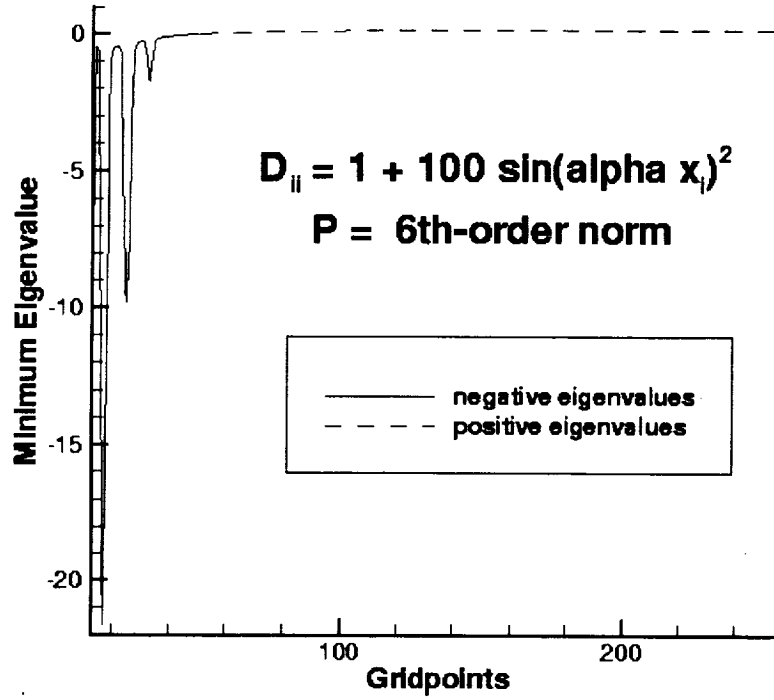
GRID REFINEMENT ON (PD +DP)

$$D_{ii} = 1 + 100 \sin(\text{alpha } x_i)^2$$
$$P = \text{6th-order norm}$$

— negative eigenvalues
- - - - positive eigenvalues

FIG. 5.3. *Minimum eigenvalue of* $PD + DP$ *as a function of* Δx.

and

$$
\begin{aligned}
BC = & (P_\xi^{-1} J_E \odot I_\eta \Sigma_1)(F - F_E) + (P_\xi^{-1} J_E \odot I_\eta \Sigma_2)(F^V - F_E^V) \\
& + (P_\xi^{-1} J_W \odot I_\eta \Sigma_3)(F - F_W) + (P_\xi^{-1} J_W \odot I_\eta \Sigma_4)(F^V - F_W^V) \\
& + (I_\xi \Sigma_5 \odot P_\eta^{-1} J_N)(G - G_N) + (I_\xi \Sigma_6 \odot P_\eta^{-1} J_N)(G^V - G_N^V) \\
& + (I_\xi \Sigma_7 \odot P_\eta^{-1} J_S)(G - G_S) + (I_\xi \Sigma_8 \odot P_\eta^{-1} J_S)(G^V - G_S^V).
\end{aligned}
\tag{5.12}
$$

The $N \times N$ matrix Q_ξ and the $M \times M$ matrix Q_η are defined in Section 3.1. Fluxes with subscripts E, W, N, S are boundary data. The matrices $\Sigma_1 - \Sigma_8$ will be determined below.

5.2.1. The energy method. Multiplying (5.10) from the left with $U^T(P_\xi \odot P_\eta)$, introducing the notation $M = P_\xi \odot P_\eta$, and adding the transpose of the equation leads to

$$
\begin{aligned}
(\|U\|_J^2)_\tau = & \underbrace{-[U^T(Q_\xi \odot P_\eta)F + F^T(Q_\xi^T \odot P_\eta)U]}_{A} + \underbrace{[U^T M h + h^T M U]}_{GR2} \\
& + \underbrace{-[U^T(P_\xi \odot Q_\eta)G + G^T(P_\xi \odot Q_\eta^T)U]}_{B} + BT + (BT)^T
\end{aligned}
\tag{5.13}
$$

where

$$
BT = U^T(J_E \odot P_\eta \Sigma_1)(F - F_E) + U^T(J_E \odot P_\eta \Sigma_2)(F^V - F_E^V)
$$

14

$$+ U^T(J_W \odot P_\eta \Sigma_3)(F - F_W) + U^T(J_W \odot P_\eta \Sigma_4)(F^V - F_W^V)$$

$$+ U^T(P_\xi \Sigma_5 \odot J_N)(G - G_N) + U^T(P_\xi \Sigma_6 \odot J_N)(G^V - G_N^V)$$

(5.14)
$$+ U^T(P_\xi \Sigma_7 \odot J_S)(G - G_S) + U^T(P_\xi \Sigma_8 \odot J_S)(G^V - G_S^V).$$

In (5.13) we have assumed that the metric transformation is such that MJ is a norm. Note that the flux terms with subscripts are given data.

The notations and abbreviations

(5.15)
$$Q_\xi + Q_\xi^T = B_\xi = J_E - J_W, \quad Q_\eta + Q_\eta^T = B_\eta = J_N - J_S,$$

will be used to expand the A and B in (5.13). We obtain

$$\text{A+B} = - \underbrace{[U^T(B_\xi \odot P_\eta)(F^I + 2F^V) + (F^I + 2F^V)^T(B_\xi \odot P_\eta)U]/2}_{\text{E-W}}$$

$$- \underbrace{[U^T(P_\xi \odot B_\eta)(G^I + 2G^V) + (G^I + 2G^V)^T(P_\xi \odot B_\eta)U]/2}_{\text{N-S}}$$

$$- \underbrace{\{[(U, D_\xi F^I) + (D_\xi F^I, U)] - [(F^I, D_\xi U) + (D_\xi U, F^I)]\}/2}_{\text{GR1}}$$

$$- \underbrace{\{[(U, D_\eta G^I) + (D_\eta G^I, U)] - [(G^I, D_\eta U) + (D_\eta U, G^I)]\}/2}_{\text{GR1}}$$

(5.16)
$$+ \underbrace{[(D_\xi U, F^V) + (F^V, D_\xi U) + (D_\eta U, G^V) + (G^V, D_\eta U)]}_{\text{DI}}.$$

Note the close similarity of the discrete energy estimate (5.13), (5.14), (5.16) with the corresponding continuous one; see (4.27). Just as in the continuous case GR1 and GR2 will at most create an exponential time growth. To obtain an energy estimate we must determine under what conditions the dissipation (DI) is negative definite and which values we must assign to the matrices $\Sigma_1 - \Sigma_8$ to obtain bounded contributions from the boundary.

5.2.2. The numerical dissipation. The DI is

(5.17)
$$DI = (D_\xi U)^T M F^V + (F^V)^T M D_\xi U + (D_\eta U)^T M G^V + (G^V)^T M D_\eta U.$$

The relationship between the gradients and the fluxes in the continuous case are given in (4.21). In matrix formulation for the discrete case we have

(5.18)
$$\begin{bmatrix} F^V \\ G^V \end{bmatrix} = - \begin{bmatrix} B_{11} & B_{12} \\ B_{21} & B_{22} \end{bmatrix} \begin{bmatrix} D_\xi U \\ D_\eta U \end{bmatrix}.$$

where $B_{kl}(i, j) = b_{kl}(\xi_i, \eta_j)$. By introducing (5.18) into (5.17) we get

(5.19)
$$DI = - \begin{bmatrix} D_\xi U \\ D_\eta U \end{bmatrix} \begin{bmatrix} B_{11}M + MB_{11} & B_{21}M + MB_{12} \\ B_{12}M + MB_{21} & B_{22}M + MB_{22} \end{bmatrix} \begin{bmatrix} D_\xi U \\ D_\eta U \end{bmatrix}.$$

At this point we need to define $M = P_\xi \odot P_\eta$ in greater detail; we have

(5.20)
$$P_\xi = \begin{bmatrix} H_\xi^L & & & \\ & 1 & & \mathbf{0} \\ & & \ddots & \\ \mathbf{0} & & 1 & \\ & & & H_\xi^R \end{bmatrix}, P_\eta = \begin{bmatrix} H_\eta^L & & & \\ & 1 & & \mathbf{0} \\ & & \ddots & \\ \mathbf{0} & & 1 & \\ & & & H_\eta^R \end{bmatrix}.$$

We will need the following lemma.

LEMMA 3. *If the blocks H_ξ^L, H_ξ^R have the size $q \times q$, the blocks H_η^L, H_η^R have the size $r \times r$, and the matrices B_{kl} in (5.18) are constant in the first q, r points normal and adjacent to the boundary $\delta\Omega$, then the dissipation DI defined in (5.19) is negative definite.* Proof: Lemma 2 leads to

$$
\begin{bmatrix} B_{11}M + MB_{11} & B_{21}M + MB_{12} \\ B_{12}M + MB_{21} & B_{22}M + MB_{22} \end{bmatrix}
$$
$$
= \begin{bmatrix} M^{1/2} & 0 \\ 0 & M^{1/2} \end{bmatrix} \begin{bmatrix} 2B_{11} & B_{12} + B_{21} \\ B_{12} + B_{21} & 2B_{22} \end{bmatrix} \begin{bmatrix} M^{1/2} & 0 \\ 0 & M^{1/2} \end{bmatrix} > 0 \quad \square.
$$

Remark. The conditions in lemma 3 (i.e., that the matrices B_{kl} in (5.18) are constant in the first q, r points normal and adjacent to the boundary $\delta\Omega$) can be thought of as theoretically ideal conditions. In practise one approaches the ideal condition with increasing resolution, smooth coefficients b_{ij} and a smooth mesh; see the *Remark* on J in Section 5.1.

5.2.3. Stability. To obtain an energy estimate (given the negative contribution of the DI on the right-hand-side of (5.16)) we must assign values to the matrices $\Sigma_1 - \Sigma_8$ in order to obtain a bounded boundary contribution.

Let us start by estimating the terms at the EAST boundary. We have

$$
BT_E = -\{U^T[P_\eta(I/2 - \Sigma_1)]F^I + (F^I)^T[(I/2 - \Sigma_1^T)P_\eta]U\}
$$
$$
- \{U^T[P_\eta(I - \Sigma_1 - \Sigma_2)]F^V + (F^V)^T[(I - \Sigma_1^T - \Sigma_2^T)P_\eta]U\}
$$
(5.21)
$$
- [U^T P_\eta \tilde{F}_E + (\tilde{F}_E)^T P_\eta U],
$$

where $\tilde{F}_E = \Sigma_1 F_E + \Sigma_2 F_E^V$.

Obviously, the terms involving the viscous fluxes must be removed. This yields $\Sigma_2 = I - \Sigma_1$. By observing that $F^I = \Lambda_E U$ where $\Lambda_E = diag((a_1)_{Nj})$ (see (4.21) for a definition of a_1) we obtain,

$$
BT_E = -U^T[P_\eta(I/2 - \Sigma_1)]\Lambda_E + \Lambda_E(I/2 - \Sigma_1^T)P_\eta]U
$$
(5.22)
$$
- [U^T P_\eta \tilde{F}_E + (\tilde{F}_E)^T P_\eta U].
$$

Now we choose Σ_1 such that $(I/2 - \Sigma_1)\Lambda_E = |\Lambda_E|/2$. This choice and an entirely similar procedure at the other boundaries yields

(5.23)
$$
(\|U\|_J^2)_\tau \leq \sum_{I=E,W,N,S} \frac{1}{\eta_I}\|\tilde{F}_I\|_I^2 + \text{GR1} + \text{GR2} + \text{DI},
$$

where

$$
\tilde{F}_E = \Sigma_1 F_E + (I_y - \Sigma_1)F_E^V, \quad \Sigma_1 = (I_y - |\Lambda_E|\Lambda_E^{-1})/2,
$$
$$
\tilde{F}_W = \Sigma_3 F_W + (I_y - \Sigma_3)F_W^V, \quad \Sigma_3 = -(I_y + |\Lambda_W|\Lambda_W^{-1})/2,
$$
$$
\tilde{G}_N = \Sigma_5 G_N + (I_r - \Sigma_5)G_N^V, \quad \Sigma_5 = (I_r - |\Lambda_N|\Lambda_N^{-1})/2,
$$
(5.24)
$$
\tilde{G}_S = \Sigma_7 G_S + (I_r - \Sigma_7)G_S^V, \quad \Sigma_7 = -(I_r + |\Lambda_S|\Lambda_S^{-1})/2,
$$

(5.25)
$$
\Sigma_2 = I_y - \Sigma_1, \quad \Sigma_4 = -I_y - \Sigma_3, \quad \Sigma_6 = I_r - \Sigma_5, \quad \Sigma_8 = -I_r - \Sigma_7,
$$

and

$$
\eta_I = \frac{1}{2}\frac{(U, |\Lambda_I|U)_I + (|\Lambda_I|U, U)_I]}{(U, U)_I}, \quad I = E, W, N, S.
$$

The similarity of the discrete energy estimate (5.23) with the corresponding continuous one (see (4.16) and (4.32)) implies strict stability. Time-integration of (5.23) leads to an estimate of the form (2.4) if the DI has the right sign, i.e., if lemma 3 holds. We can conclude that the following theorem holds.

THEOREM 6. *The approximation (5.10) of the problem (4.20), (4.30), (4.31) is both strictly and strongly stable if lemma 3 holds and $\Sigma_1 - \Sigma_8$ are given by (5.24) and (5.25).*

5.3. The 1D multiple domain problem revisited. Before we consider the 2D multiple-domain problem, let us once more look at the 1D multiple-domain problem considered in [17], [18].

5.3.1. Derivation of the Q-formulation for interface problems. Consider the following hyperbolic interface problem

$$(5.26) \qquad u_t + u_x = 0, \quad -1 \le x \le 0, \quad \text{and} \quad v_t + v_x = 0, \quad 0 \le x \le 1$$

augmented with suitable initial and boundary data and the interface condition $u = v$ at $x = 0$. The straightforward approximation of (5.26) is

$$\begin{aligned} U_t + P_L^{-1} Q_L U &= P_L^{-1}(\sigma_L(U_N - V_0)e_N) \\ (5.27) \qquad V_t + P_R^{-1} Q_R V &= P_R^{-1}(\sigma_R(V_0 - U_N)e_0) \end{aligned}$$

where $U = (U_0, ..., U_N)^T, e_N = (0, ..., 0, 1)^T, V = (V_0, ..., V_M)^T, e_0 = (1, 0..., 0)^T$.

The boundary terms from the left (L) and right (R) outer boundaries are ignored. The formulation (5.27) can also be written in the following way:

$$(5.28) \qquad PW_t + (Q + \Sigma)W = 0$$

where $W = (U, V)^T, P = diag(P_L, P_R), Q = diag(Q_L, Q_R)$, and

$$(5.29) \qquad \Sigma = \left[\begin{array}{cc} 0 & 0 \\ & \tilde{\Sigma} & \\ 0 & 0 \end{array} \right], \quad \tilde{\Sigma} = \left[\begin{array}{cc} -\sigma_L & +\sigma_L \\ +\sigma_R & -\sigma_R \end{array} \right].$$

We can now split up $Q + \Sigma$ into a symmetric and a skew-symmetric part as

$$Q + \Sigma = \underbrace{\frac{(Q + \Sigma) - (Q + \Sigma)^T}{2}}_{Q^{sk}} + \underbrace{\frac{(Q + \Sigma) + (Q + \Sigma)^T}{2}}_{D}.$$

The 2×2 blocks of Q^{sk} and D corresponding to the nonzero elements in Σ are

$$\tilde{Q}^{sk} = \frac{1}{2} \left[\begin{array}{cc} 0 & (\sigma_L - \sigma_R) \\ -(\sigma_L - \sigma_R) & 0 \end{array} \right], \quad \tilde{D} = \frac{1}{2} \left[\begin{array}{cc} 1 - 2\sigma_L & \sigma_L + \sigma_R \\ \sigma_L + \sigma_R & -1 - 2\sigma_R \end{array} \right].$$

In the sequel, the "tilde" sign will indicate the 4×4 block that couples the solutions in the left and right domains. Equation (5.28) now becomes

$$(5.30) \qquad PW_t + (Q^{sk} + D)W = 0.$$

In [17] it was shown that (5.27) is conservative if $\sigma_R = \sigma_L - 1$. By introducing this condition in $\tilde{Q}^{sk}$ and $\tilde{D}$ we obtain the final form of the difference operator

$$(5.31) \qquad \tilde{Q}^{sk} = \frac{1}{2} \left[\begin{array}{cc} 0 & 1 \\ -1 & 0 \end{array} \right], \quad \tilde{D} = \sigma \left[\begin{array}{cc} 1 & -1 \\ -1 & 1 \end{array} \right].$$

17

where $\sigma = 1/2 - \sigma_L$.

The formulation (5.30), (5.31) hereafter referred to as the Q-formulation is a rearranged form of the original formulation (5.27). However, the Q-formulation simplifies and even extends the possibility to formulate suitable penalty terms for second order derivatives.

5.3.2. The Q-formulation for advection-diffusion interface problems. Consider

$$(5.32) \qquad u_t + F(u)_x = 0, \quad -1 \le x \le 0, \quad \text{and} \quad v_t + F(v)_x = 0, \quad 0 \le x \le 1$$

where $F(w) = a(x,t)w - \epsilon w_x$ augmented with suitable initial, boundary, and interface conditions. An approximation of (5.32) using the Q-formulation is

$$(5.33) \qquad PW_t + (Q^{sk})(AW) - \epsilon(Q^{sk} + D_2)P^{-1}(Q^{sk} + D_3) = D_1 W$$

where $W = (U, V)^T$ and $P = diag(P_L, P_R)$. The matrix A has the values of $a(x_i, t)$ on the diagonal. The operator Q^{sk} is defined in the previous Section, and

$$(5.34) \qquad \tilde{D}_i = \sigma_i \begin{bmatrix} 1 & -1 \\ -1 & 1 \end{bmatrix}, \quad i = 1, 2, 3$$

as in (5.31). The dissipation D_1 is formulated as acting on W, which is a more general formulation that includes penalty on the flux ($\sigma_1 = \sigma a(0, t)$) as well as penalty on the variables.

We can now prove

THEOREM 7. *The approximation (5.33), (5.34) of the problem (5.32) with the choices*

$$(5.35) \qquad \sigma_1 \le 0, \quad \sigma_2 = 0, \quad \sigma_3 = 0$$

is conservative and stable.

Proof: The energy method applied on (5.33) leads to

$$\|W\|_t^2 = \underbrace{(\mathcal{D}W, AW) - (\mathcal{D}(AW), W)}_{GR1} - \underbrace{2\epsilon(\mathcal{D}W, \mathcal{D}W)}_{DI} - \underbrace{W^T B(AW - 2\epsilon\mathcal{D}W)}_{BT} + \text{IT}$$

where $\mathcal{D}W = P^{-1}Q^{sk}W$ and the interface terms IT are defined as

$$(5.36) \qquad IT = \begin{bmatrix} W \\ \mathcal{D}W \end{bmatrix}_0^T \begin{bmatrix} 2D_1 + 2\epsilon D_2 P^{-1} D_3 & \epsilon(D_2 - D_3) \\ \epsilon(D_2 - D_3) & 0 \end{bmatrix} \begin{bmatrix} W \\ \mathcal{D}W \end{bmatrix}_0.$$

The growth (GR1), the dissipation (DI) and the ordinary boundary terms (BT) match the terms in the corresponding continuous estimate perfectly. The choices (5.35) makes the term IT maximally negative definite and leads to stability. The approximation (5.33) can now can be written

$$(5.37) \qquad PW_t + Q^{sk}(AW - \epsilon P^{-1}Q^{sk}W) = D_1 W,$$

which leads to conservation. $\square$

It remains to identify the penalty terms and corresponding interface conditions and find out whether (5.37) is sufficiently accurate. The equation

$$PW_t + Q(AW - \epsilon P^{-1}QW) = (D_1 + (Q - Q^{sk})A)W + \epsilon(Q^{sk}P^{-1}Q^{sk} - QP^{-1}Q)W$$
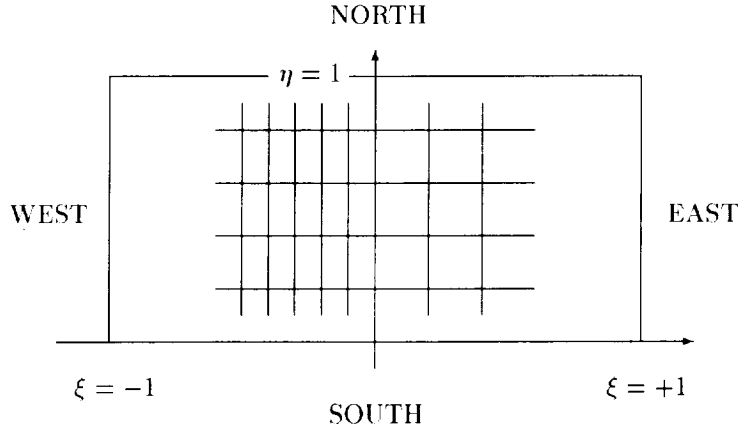
FIG. 5.4. *The multiple domain mesh in transformed space.*

is a formulation of (5.37) in the usual penalty form. Obviously, the penalty terms (denoted by PT) indicate that the one-sided first and second derivatives are replaced by first and second derivatives involving the adjacent domain, and that dissipation is introduced via D_1.

By introducing

$$Q^{sk} - Q = \Delta, \quad \tilde{\Delta} = -\frac{1}{2}\begin{bmatrix} 1 & -1 \\ 1 & -1 \end{bmatrix}, \quad \tilde{\Lambda} = \begin{bmatrix} -(2\sigma_1 + a) & 0 \\ 0 & (2\sigma_1 - a) \end{bmatrix}$$

we get PT $= \Lambda\Delta W + \epsilon(\Delta(P^{-1}QW) + Q^{sk}\Delta W)$; this result shows that the corresponding interface conditions are $u = v$ and $u_x = v_x$. Also, because

$$\tilde{\Delta}\phi = (0,0)^T, \quad \tilde{\Delta}(P^{-1}Q\phi) = (\mathcal{O}(\Delta x_L^{r-1}, \Delta x_R^{r-1}), \mathcal{O}(\Delta x_L^{r-1}, \Delta x_R^{r-1}))^T$$

where ϕ is a smooth function and r is the order of the approximation at inner points, the approximation (5.37) is accurate enough.

5.4. The 2D multiple-domain problem. In this Section, an interface at $\xi = 0$ with matching gridlines (see Figure 5.4) is considered. Matching gridlines implies that the number of points in the η direction (M) is the same on both sides of $\xi = 0$. We will also assume that $P_\eta^L = P_\eta^R = P_\eta$, which implies that $Q_\eta^L = Q_\eta^R = Q_\eta$. Note that, in general, the difference operators D_ξ^L, D_ξ^R can be different in the left and right domains and that $\Delta\xi_L \neq \Delta\xi_R$ and $N_L \neq N_R$.

A multiple-domain Q-formulation of the problem (4.20), (4.30), (4.31) is

$$(5.38) \qquad \bar{J}W_t + D_\xi^{sk}F + D_\eta G = \bar{M}^{-1}(D \cdot \Sigma P_\eta)W + h + \text{BC}, \quad W(0) = f$$

where $W = (U, V)^T$. The solutions in the left (L) and right (R) domains are denoted respectively by U and V, and

$$(5.39) \qquad D_\xi^{sk} = \bar{M}^{-1}(Q_\xi^{sk} \cdot P_\eta), \quad D_\eta = \bar{M}^{-1}(P_\xi \cdot Q_\eta).$$

In (5.38), BC denotes the boundary conditions in (5.10) at the NORTH, EAST, SOUTH, WEST boundaries in penalty form, h is the forcing function, f the initial data, and $F = F^I + F^V$, $G = G^I + G^V$ the fluxes where

$$(5.40) \qquad i.eoF^I = A_1 W, \quad F^V = -(B_{11}D_\xi^{sk}W + B_{12}D_\eta W),$$

19

(5.41) $$G^I = A_2 W, \quad G^V = -(B_{21} D_\xi^{sk} W + B_{22} D_\eta W).$$

The remaining definitions and notations used in (5.38) are $\bar{Q}_\xi^{sk} = \bar{Q}_\xi + \Delta$,

(5.42) $$\bar{M} = \begin{bmatrix} M_L & 0 \\ 0 & M_R \end{bmatrix}, \quad \bar{J} = \begin{bmatrix} J_L & 0 \\ 0 & J_R \end{bmatrix}, \quad \bar{Q}_\xi = \begin{bmatrix} Q_\xi^L & 0 \\ 0 & Q_\xi^R \end{bmatrix},$$

(5.43) $$\Delta = \begin{bmatrix} 0 & & 0 \\ & \tilde{\Delta} & \\ 0 & & 0 \end{bmatrix}, \quad D = \begin{bmatrix} 0 & & 0 \\ & \tilde{D} & \\ 0 & & 0 \end{bmatrix},$$

.(5.44) $$\bar{P}_\xi = \begin{bmatrix} P_\xi^L & 0 \\ 0 & P_\xi^R \end{bmatrix}, \quad \tilde{\Delta} = -\frac{1}{2}\begin{bmatrix} 1 & -1 \\ 1 & -1 \end{bmatrix}, \quad \tilde{D} = \begin{bmatrix} 1 & -1 \\ -1 & 1 \end{bmatrix}.$$

The matrix coefficient Σ will be determined by stability requirements.

5.4.1. Conservation. The Q-formulation automatically leads to conservation:

THEOREM 8. *The approximation (5.38) of (4.20), (4.30), (4.31) is conservative.*

Proof: Let $h = BC = 0$. Multiplying (5.38) with the integration operator $\phi^T \bar{M}$ where ϕ is smooth, and observing that $Q_\xi^{sk} = -(Q_\xi^{sk})^T + B_\xi$, $Q_\eta = -Q_\eta^T + B_\eta$ (B_ξ, B_η are defined in (5.15)) leads directly to

$$\phi^T \bar{M} \bar{J} W_t - (D_\xi^{sk}\phi)^T \bar{M} F - (D_\eta\phi)^T \bar{M} G + \phi^T (B_\xi \odot P_\eta)F + \phi^T (P_\xi \odot B_\eta)G = 0.$$

The approximation (5.38) is conservative; i.e., it reverses the process of differentiation (second and third terms above) and leaves information only at the boundaries (fourth and fifth terms). $\square$

5.4.2. Stability. In this Section we will prove the following theorem.

THEOREM 9. *The approximation (5.38) of the problem (4.20), (4.30), (4.31) is both strictly and strongly stable if theorem 6 holds and $\Sigma P_\eta + P_\eta \Sigma \leq 0$.*

Proof: The energy method applied to (5.38) yields

(5.45) $$\frac{d}{dt}(\|W\|_J^2) = GR1 + GR2 + DI + BT_E + BT_W + BT_N + BT_S + IT$$

where it is assumed that $\bar{M}\bar{J}$ is a norm; the requirements are given in theorem 5. The boundary terms $BT_E + BT_W + BT_N + BT_S$ are exactly the same as in the single domain case (see (5.24)), while the D_ξ operator in GR1, GR2, and DI is replaced by D_ξ^{sk} defined in (5.39). Strict and strong stability of (5.38) follows if

(5.46) $$IT = W^T D \odot (\Sigma P_\eta + P_\eta \Sigma)W \leq 0.$$

Because $D \geq 0$, we need $\Sigma P_\eta + P_\eta \Sigma \leq 0$. $\square$

Remark. Because $P_\eta > 0$, $\Sigma \leq 0$ with the first and last r elements in Σ being constants would satisfy condition (5.46).

6. Numerical experiments. In the calculations below, we have used the fourth- and sixth-order schemes reported in [17] in space and a five-stage fourth-order RK scheme [32] in time.
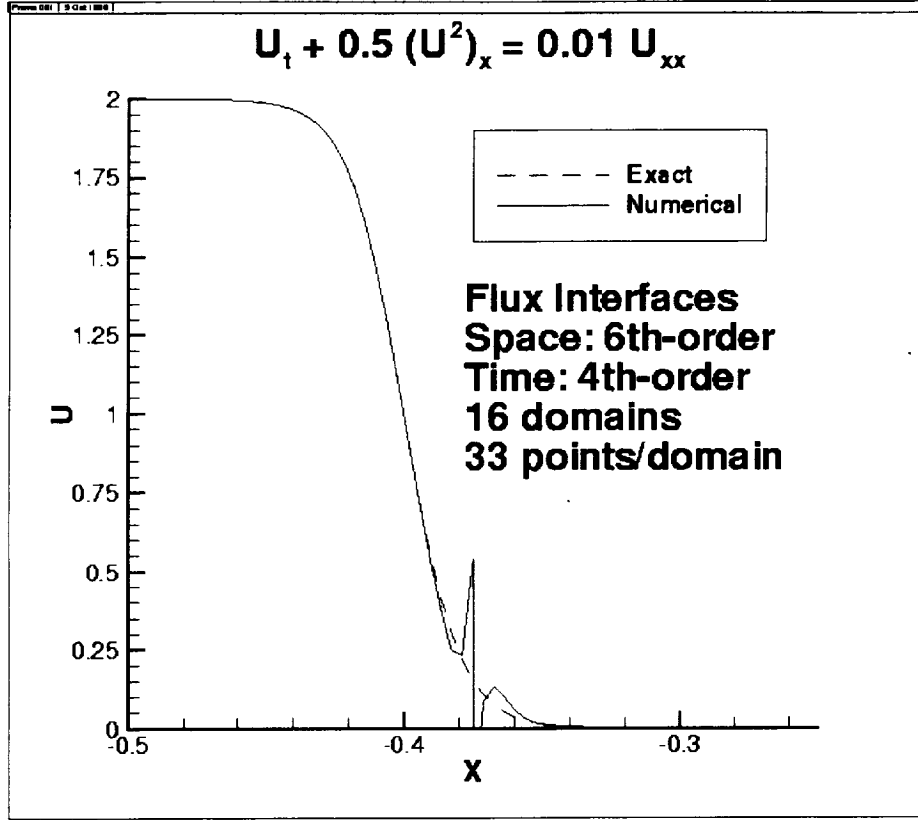
$$U_t + 0.5\,(U^2)_x = 0.01\,U_{xx}$$

- - - - Exact
———— Numerical

**Flux Interfaces
Space: 6th-order
Time: 4th-order
16 domains
33 points/domain**

FIG. 6.1. *Instability due to vanishing wave speed and flux interface conditions.*

6.1. Vanishing wave speed.

For problems with a realistic geometry, one will frequently encounter zero wave speed somewhere in the field due to the variation of the metric coefficients, the variable coefficients, or (for nonlinear problems) the solution. This difficulty (see Section 4.3.2) particularly severe in one dimension, is exemplified in the calculation of Burger's equation shown in Figure 6.1.

The instability that develops close to zero wave speed when using a penalty on the fluxes at the interfaces is evident. With interface conditions applied on the variable instead of the fluxes, the instability disappears. Also, if one scales the problem such that U varies between 1 and 3 instead of 0 and 2 one can use flux interface conditions without any sign of instabilities. This anomalous behavior associated with a vanishing wave speed occurs with other numerical schemes, and is typically suppressed by adding dissipation (e.g. the "Entropy fix" used with Roe solvers).

6.2. Error growth due to varying coefficients.

Consider the following 1D test problem,

$$(6.1) \qquad \begin{aligned} u_t + F_x &= 0, \quad [x, y] \in \Omega, \quad t \geq 0 \\ u &= f, \quad [x, y] \in \Omega, \quad t = 0 \end{aligned}$$

on the 2D domain $\Omega = [x, y] \in [0, 1] \times [0, 1]$. The variables, fluxes and initial data are

$$(6.2) \qquad u = \begin{bmatrix} u_1 \\ u_2 \end{bmatrix}, \quad F = \begin{bmatrix} a(x)u_1 \\ b(x)u_2 \end{bmatrix}, \quad f = \begin{bmatrix} \sin(2\pi x) \\ \sin(2\pi x) \end{bmatrix}.$$
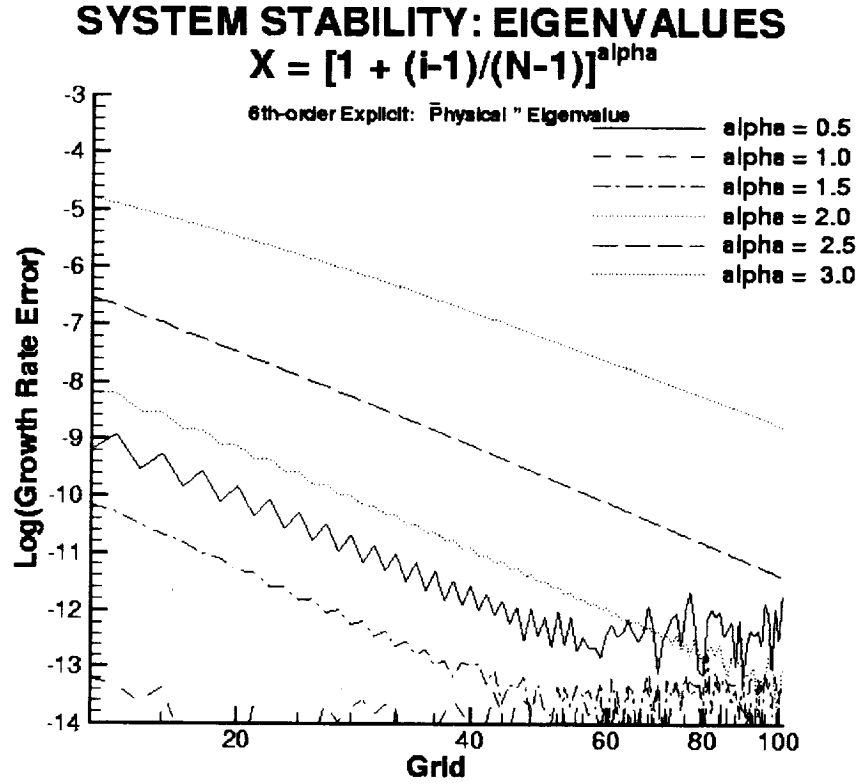
FIG. 6.2. *The error in the growth rate for different transformations.*

The problem (6.1) is 1-periodic in y and has

(6.3) $$u_1(0, y, t) = \alpha u_2(0, y, t), \quad u_2(1, y, t) = \beta u_1(1, y, t),$$

as boundary conditions in the x-direction.

By introducing a 2D curvilinear mesh we obtain

(6.4) $$\begin{aligned} Ju_\tau + (F)_\xi + (G)_\eta &= ,0 \quad [\xi, \eta] \in \Omega, \quad \tau \geq 0 \\ u &= f, \quad [\xi, \eta] \in \Omega, \quad \tau = 0 \end{aligned}$$

where $F = J\xi_x F, G = J\eta_x F$ and $\Omega = [\xi, \eta] \in [0, 1] \times [0, 1]$. The problem (6.4) has the same boundary conditions as (6.1).

6.2.1. The energy growth in 1D. The energy growth for the 1D $(y = 0, \eta_x = 0)$ version of (6.1)-(6.4) with

(6.5) $$a = 1 + \epsilon x, \quad b = -1 + \epsilon x, \quad \alpha = 1, \quad \beta = \sqrt{(1 + \epsilon)/(1 - \epsilon)}$$

leads to $\|u\|_t^2 = -\epsilon\|u\|^2$. The growth rate $-\epsilon/2$ corresponds to a single eigenvalue on the real axis in the continuous spectrum. Figure 6.2 shows the error in the sixth-order numerical approximation of this eigenvalue for different transformations $(x = x(\xi))$. Figure 6.3 shows the convergence (in an L_2 sense) of the seven eigenvalues with most accurately converged real parts. The convergence rate in both Figures 6.2 and 6.3 is at least 6.

SYSTEM STABILITY: EIGENVALUES
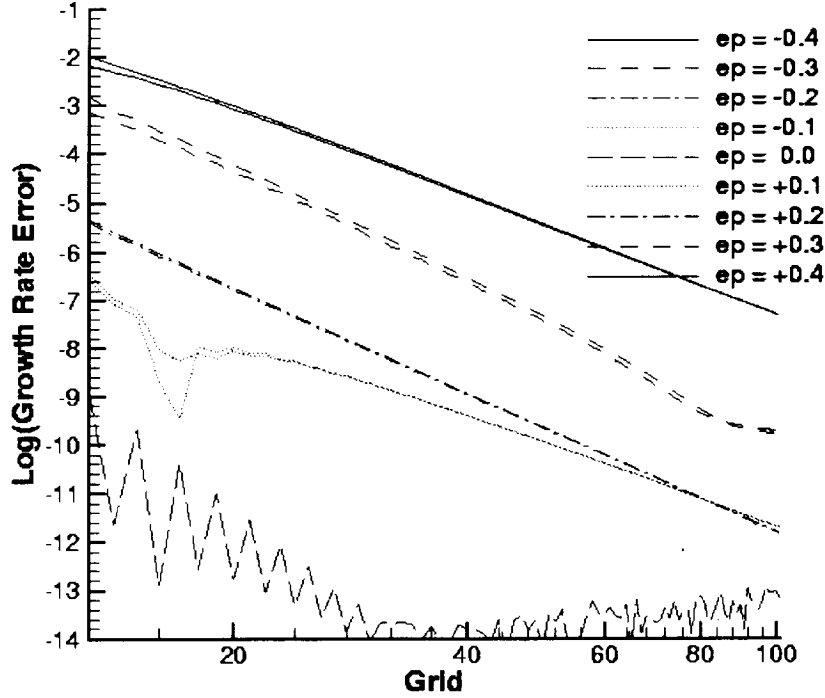
Seven Most-Accurate Eigenvalues

FIG. 6.3. *The error in the growth rate for varying wave speeds.*

Even though the resolved eigenvalues (and eigenvectors) converge at the theoretical rate (see Figures 6.2-6.3), there are unresolved eigenvalues and eigenvectors that can generate difficulties. In Figure 6.4, the least resolved eigenvector corresponds to an eigenvalue with a negative real part (-4.6529E-03) significantly more to the right of the analytical value (-7.5000E-03) than could be expected by the order of the approximation. These unresolved eigenvalues and eigenvectors may generate extra large energy growth, as shown in Figure 6.5. The growth varies with the initial condition. Note that the extra energy growth for a uniform mesh can be present only for varying coefficients because otherwise $GR1 = (F, D_r U) - (D_r F, U) \equiv 0$.

6.2.2. The energy growth in 2D.

The energy growth for the 2D continuous problems (6.1), (6.4) is identically zero with $\epsilon = 0$ in (6.5); i.e., the L_2 norm of the solution remains constant in time. In the semi-discrete case, the energy growth is given by (5.45) where $GR2 = DI = 0$ and the introduction of boundary conditions (BT_I) and interface conditions (IT) leads to damping. Possible error growth, see (5.16), is provided by,

$$(6.6) \qquad GR1 = -[(U, D_\xi F) - (D_\xi U, F)] - [(U, D_\eta G) - (D_\eta U, G)]$$

only. For a linear mapping where the metric coefficients are constants (see Figure 6.6) we obtain $D_\xi F = D_\xi \Lambda_1 U = \Lambda_1 D_\xi U, D_\eta G = D_\eta \Lambda_2 U = \Lambda_2 D_\eta U$, which yields $GR1 = 0$. The error growth is shown in Figure 6.7. The calculations are fourth-order accurate in time. Note that there is an absolute bound on the error.

In a nonlinear mapping (see Figure 6.8) the truncation errors in the metric calculation, and consequently also in the calculation of the fluxes, leads to $GR1 \neq 0$, which in turn can generate error growth (see Figure

SYSTEM STABILITY: EIGENVECTORS

Physical, First, and Re(max)

Legend:
- □ -7.5000E-03, 0.0
- △ -7.5007E-03, -3.140518
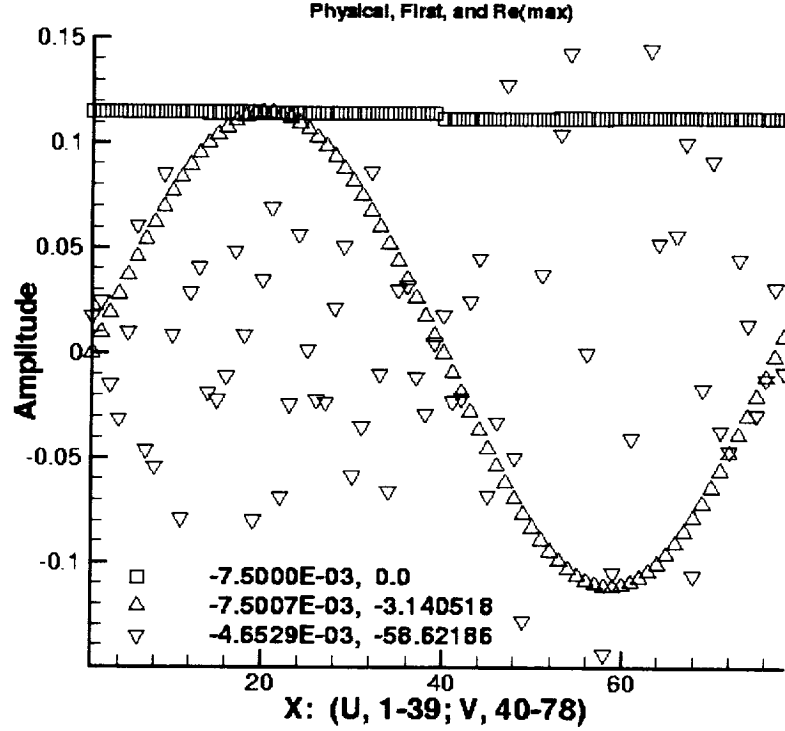- ▽ -4.6529E-03, -56.62186

X: (U, 1-39; V, 40-78)

FIG. 6.4. *Eigenvectors related to two most and least resolved eigenvalues.*

6.9). These calculations also are fourth-order accurate in time. Note the enormous time scale in Figures 6.7, and 6.9.

6.3. Navier-Stokes calculations. We consider here a 1D viscous shock propagating in accordance with a Mach number of 2.0 and a Reynolds number 150 over a 2D domain. The exact solution of the Navier-Stokes equation for this case can be found in [33]. At the artificial boundaries, including the circular region in the middle, we impose flux boundary conditions by using the penalty formulation on the fluxes with exact data from the analytical solution. At the interfaces we impose interface conditions by using the penalty formulation on the variables.

In Figure 6.10, the density and grid for the propagating shock is shown. The shock travels from the lower left corner to the upper right corner and has almost passed out of the computational domain that consists of 12 blocks. The sixth order scheme and 24 gridpoints were used in each sub-domain. The local density errors are shown in Figure 6.11. The grid refinement study in Table 6.3 indicate between fifth- and sixth-order accuracy in an L_2 norm, consistent with the theory in [34], [35], since we have fifth order accuracy at the boundaries and interfaces (see (3.4)) and relatively coarse grids.

7. Summary and conclusions. We have analyzed boundary and interface conditions for high order finite difference methods applied to multidimensional linear problems in curvilinear coordinates. The investigation focused on the effect of variable coefficients.

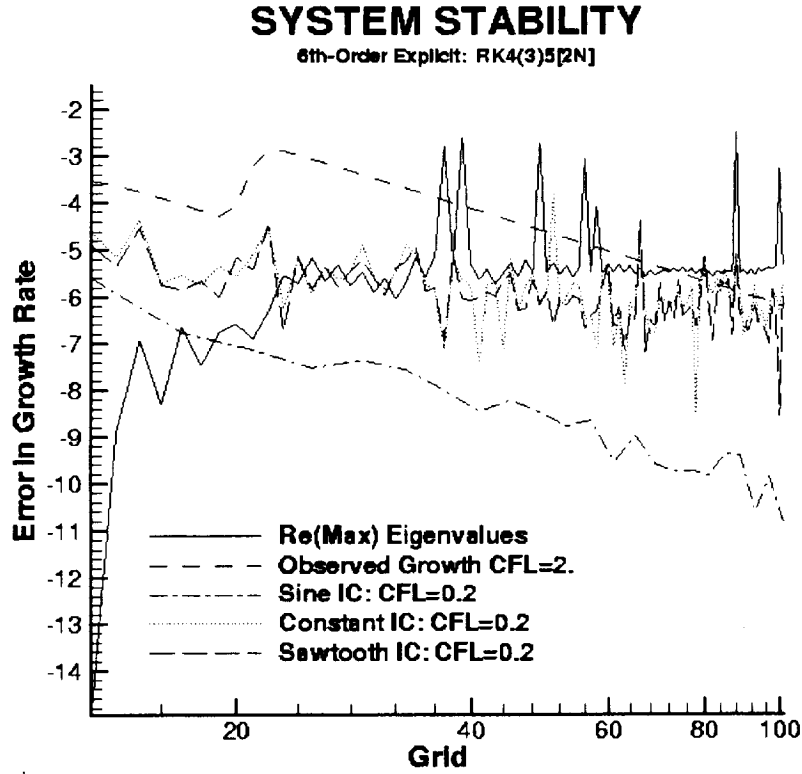A problem with a norm as a function of the Jacobian was analyzed. Boundary and interface conditions

SYSTEM STABILITY

6th-Order Explicit: RK4(3)5[2N]

FIG. 6.5. *Extra growth due to unresolved features and initial conditions.*

TABLE 6.1

Twelve subdomains, sixth-order explicit; CFL = 0.3.

Wave speed	49/65	65/97	97/129	129/193
-0.25	-4.610	-4.640	-4.722	-4.722
0.00	-5.115	-4.986	-4.538	-4.657
0.25	-5.155	-5.253	-5.179	-4.952
0.50	-5.331	-5.401	-5.467	-5.327
0.75	-5.523	-5.514	-5.590	-5.565
1.00	-5.635	-5.622	-5.659	-5.719
average	-5.228	-5.236	-5.193	-5.196

in both flux and variable formulations have been investigated. Flux boundary conditions lead to energy estimates whereas flux interface conditions lead to difficulties if the wave speed approaches zero.

A new and simplified so called Q-formulation of the penalty method was derived at interfaces. The Q-formulation simplifies and extends the formulation and implementation of derivative conditions in both one and two dimensions at interfaces.

It was shown that varying coefficients can cause unbounded error growth via the truncation errors even though the boundary and interface conditions are implemented in a stable and dissipative way. The error growth may be large due to unresolved features in the solution. Numerical calculations confirmed the
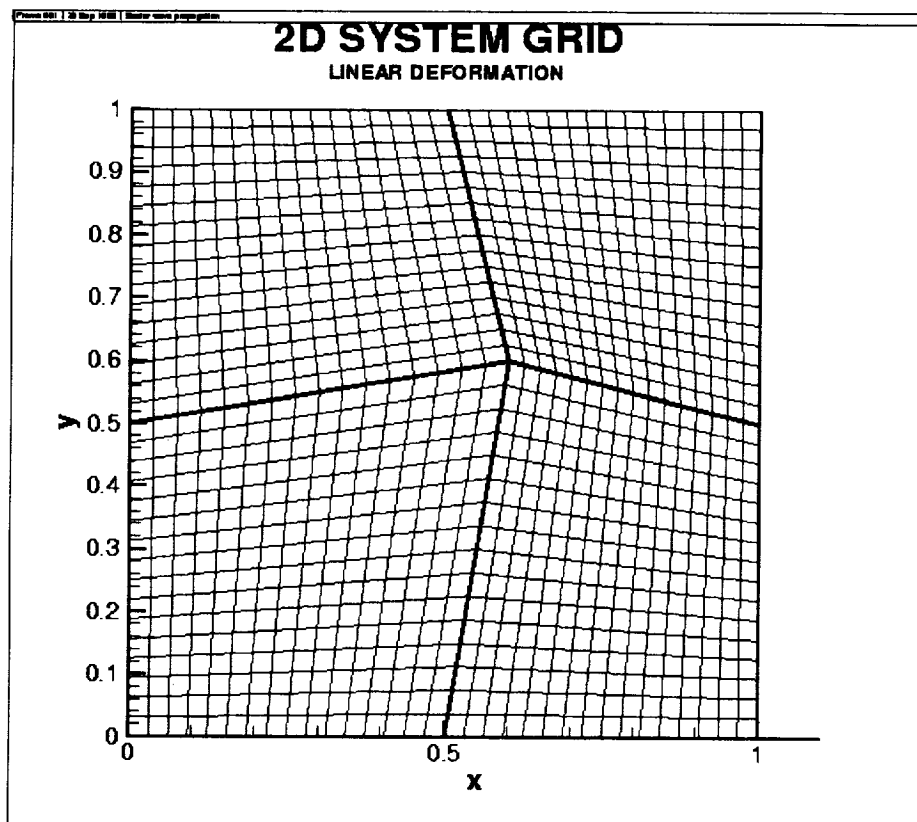
25

2D SYSTEM GRID

LINEAR DEFORMATION

FIG. 6.6. *A 4 block mesh, linear mapping.*

theoretical conclusions.

REFERENCES

[1] R.L. CLARK AND K.D. FRAMPTON, *Aeroelastic structural acoustic coupling: Implications on the control of turbulent boundary-layer noise transmission*, J. Acoust. Soc. Amer., 102, (1997), pp. 1639-1647.

[2] D.-L. LIU AND R.C. WAAG, *Harmonic amplitude distribution in a wideband ultrasonic wavefront after propagation through human abdominal wall and breast specimens*, J. Acoust. Soc. Amer., 101, (1997), pp. 1172-1183.

[3] M. LOU AND J.A. RIAL, *Characterization of geothermal reservoir crack patterns using shear-wave splitting*, Geophysics, 62, (1997), pp. 487-494.

[4] M. OKONIEWSKI AND M.A. STUCHLY, *A study of the handset antenna and human body interaction*, IEEE Trans. Microwave Theory Tech., 44, (1996), pp. 1855-1864.

[5] C. TAM AND J. WEBB, *Dispersion-Relation-Preserving Finite Difference Schemes for Computational Acoustics*, J. Comput. Phys., 107, No. 2, (1993), pp. 262-281.

[6] C. PRUETT, T. ZANG, C. CHANG AND M.H. CARPENTER, *Spatial Direct Numerical Simulation of High Speed Boundary-Layer Flows, Part 1: Algorithmic Considerations and Validation*, Theoretical and Computational Fluid Dynamics, 7, (1995).

[7] H.O. KREISS AND J. OLIGER, *Comparison of Accurate Methods for the Integration of Hyperbolic Equa-*
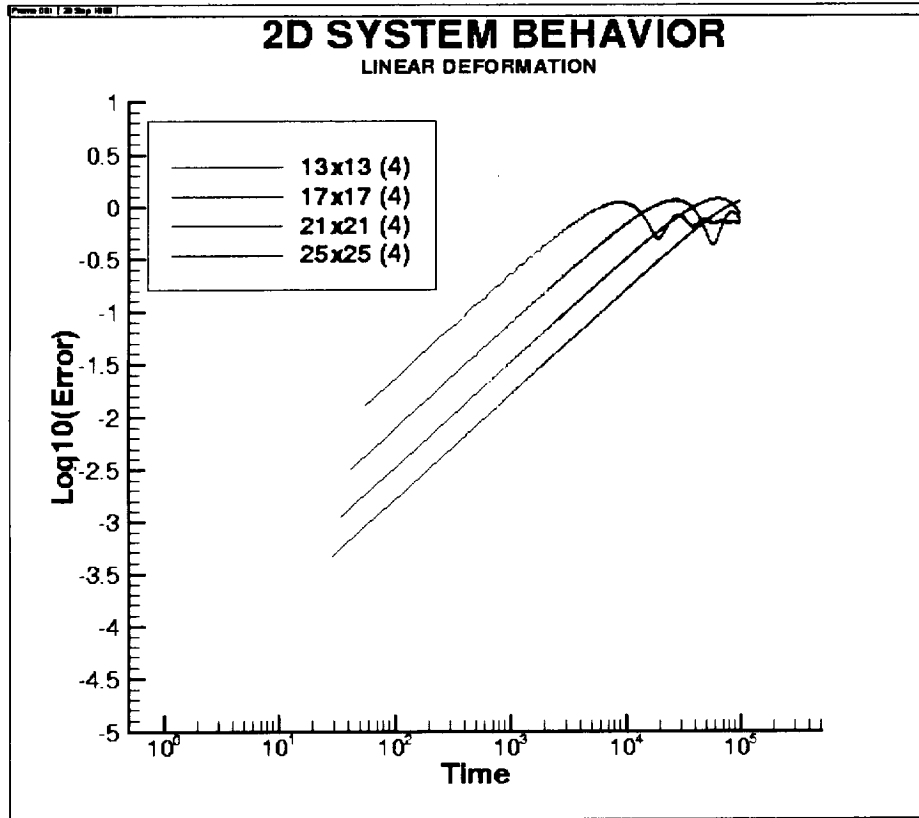
FIG. 6.7. *Growth rates, linear mapping.*

tions, Tellus XXIV, 3, (1972).

[8] G. SCHERER, *On Energy Estimates for Difference Approximations to Hyperbolic Partial Differential Equations*, PhD Thesis, Department of Scientific Computing, Uppsala University, 1977.

[9] H.O. KREISS AND G. SCHERER, *Finite element and finite difference methods for hyperbolic partial differential equations*, Mathematical Aspects of Finite Elements in Partial Differential Equations. Academic Press, New York, 1974.

[10] P. OLSSON, *High-order difference methods and data-parallel implementation*, PhD Thesis. Uppsala University, Department of Scientific Computing, 1992.

[11] B. STRAND, *High-Order Difference Approximations for Hyperbolic Initial Boundary Value Problems*, PhD Thesis, Uppsala University. Department of Scientific Computing, 1996.

[12] B. STRAND, *Summation by Parts for Finite Difference Approximations for d/dx*, J. Comput. Phys., 110, No. 1, (1994), pp. 47-67.

[13] P. OLSSON, *Summation by Parts, Projections, and Stability I*, Math. Comp., 64, (1995), pp. 1035-1065.

[14] P. OLSSON, *Summation by Parts, Projections, and Stability II*, Math. Comp., 64, (1995), pp. 1473-1493.

[15] M.H. CARPENTER, D. GOTTLIEB AND S. ABARBANEL. *The Stability of Numerical Boundary Treatments for Compact High-Order Finite-Difference Schemes*, J. Comput. Phys., 108, No. 2, (1994), pp. 272-295.

[16] M.H. CARPENTER, D. GOTTLIEB AND S. ABARBANEL, *Time-Stable Boundary Conditions for Finite-Difference Schemes Solving Hyperbolic Systems: Methodology and Application to High-Order Com-*
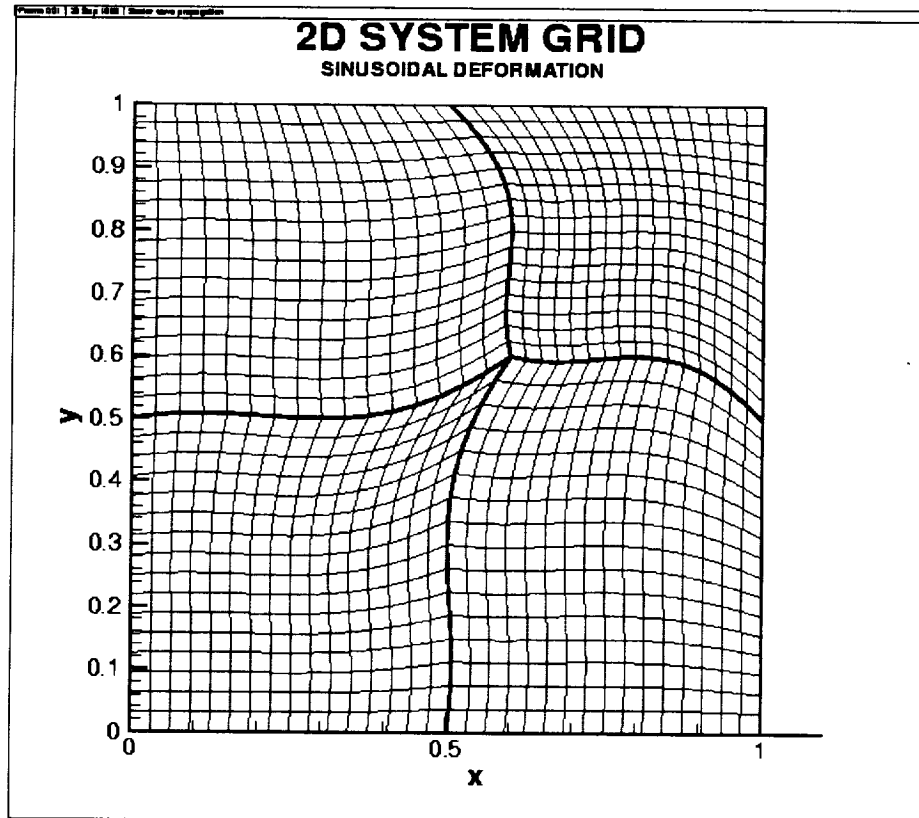
FIG. 6.8. *A four-block mesh, nonlinear mapping.*

pact Schemes, J. Comput. Phys., 111, No. 2, (1994), pp. 220-236.

[17] M.H. CARPENTER, J. NORDSTRÖM AND D. GOTTLIEB, *A Stable and Conservative Interface Treatment of Arbitrary Spatial Accuracy*, J. Comput. Phys., 148, No. 2, (1999), pp. 341-365.

[18] J. NORDSTRÖM AND M.H. CARPENTER, *Boundary and Interface Conditions for High Order Finite Difference Methods Applied to the Euler and Navier-Stokes Equations*, J. Comput. Phys., 148, No. 2, (1999), pp. 621-645.

[19] D.A. KOPRIVA, *Spectral methods for the Euler Equations, the Blunt Body Problem Revisited*, AIAA J., 29, (1991), pp. 1458-1462.

[20] J.S. HESTHAVEN AND D. GOTTLIEB, *A Stable Penalty Method for the Compressible Navier-Stokes Equations: 1. Open Boundary Conditions*, SIAM J. Sci. Comput., 17. No. 3, (1996), pp. 579-612.

[21] J.S. HESTHAVEN, *A Stable Penalty Method for the Compressible Navier-Stokes Equations: II. One-Dimensional Domain Decomposition Schemes*, SIAM J. Sci. Comput., 18, No. 3, (1997), pp. 658-685.

[22] B. SJÖGREN, *High-Order Centered Difference Methods for the Compressible Navier-Stokes Equations*, J. Comput. Phys., 117, No. 2, (1995), pp. 251-261.

[23] J. HYMAN, M. SHASHKOV, J. CASTILLO AND S. STEINBERG, *High Order Mimetic Finite Difference Methods on Nonuniform Grids*, Proceedings from ICOSAHOM 95, paper 11, (1995).

[24] B. GUSTAFSSON, H.O. KREISS AND J. OLIGER, *Time Dependent Problems and Difference Methods*, John Wiley and Sons, 1996.

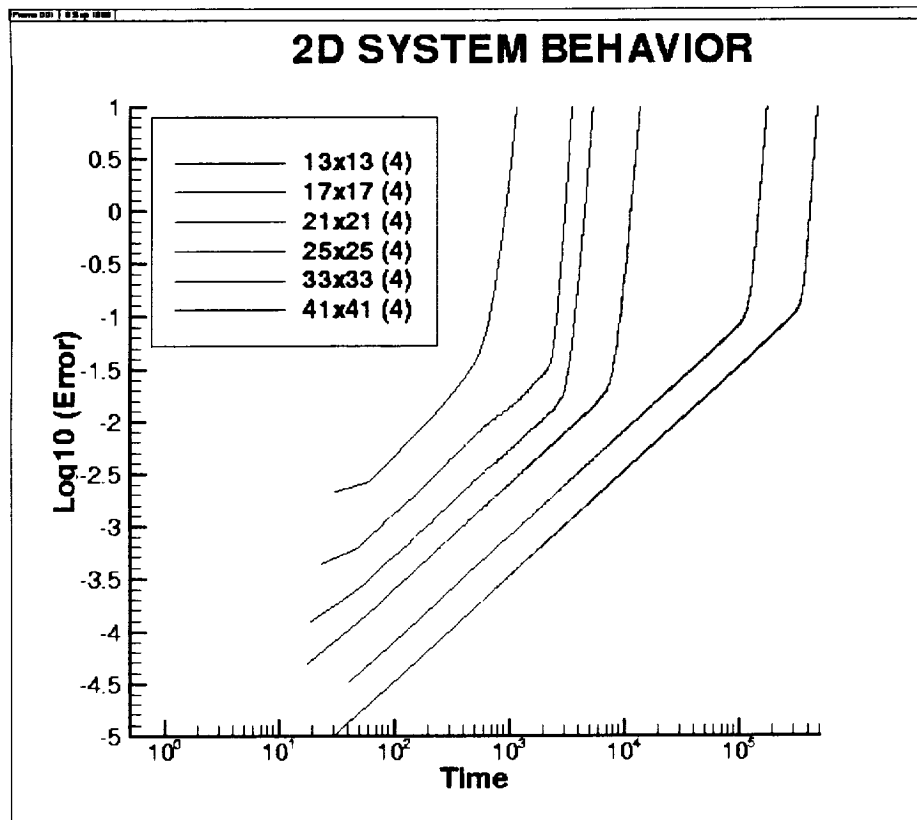[25] C. VAN LOAN, *Computational Frameworks for the Fast Fourier Transform*, Society for Industrial and

FIG. 6.9. *Growth rates, nonlinear mapping.*

Applied Mathematics, Philadelphia, 1992.

[26] M.H. CARPENTER AND J. OTTO, *High-Order Cyclo-Difference Techniques: An Alternative to Finite Differences*, J. Comput. Phys., 118, (1995), pp. 242-260.

[27] J. NORDSTRÖM, *On Flux-Extrapolation at Supersonic Outflow Boundaries*, Applied Numerical Mathematics, 30. Issue 4, (1999), pp. 447-457.

[28] S.N. BERNSTEIN, *Demonstration du theoreme de Weistrass fondee sur le calcul de probalite*, Proceedings of the Mathematical Society of Kharkov. XIII, (1912).

[29] J. NORDSTRÖM, *The Use of Characteristic Boundary Conditions for the Navier-Stokes Equations*, Computers & Fluids. 24. No. 5, (1995), pp. 609-623.

[30] H.O. KREISS AND J. LORENZ, *Initial Boundary Value Problems and the Navier-Stokes Equations*, Academic Press. 1989.

[31] J. NORDSTRÖM, *The Influence of Open Boundary Conditions on the Convergence to Steady State for the Navier-Stokes Equations*, J. Comput. Phys., 85 (1989), pp. 210-244.

[32] M.H. CARPENTER AND C.A. KENNEDY, *Fourth-Order 2N-Storage Runge-Kutta Schemes*, NASA-TM-109111, April 1994.

[33] F.M. WHITE, *Viscous Fluid Flow*, McGraw-Hill, New York, 1974.

[34] B. GUSTAFSSON, *The Convergence Rate for Difference Approximations to Mixed Initial Boundary Value Problems*, Math. Comp., 29, (1975), pp. 396-406.

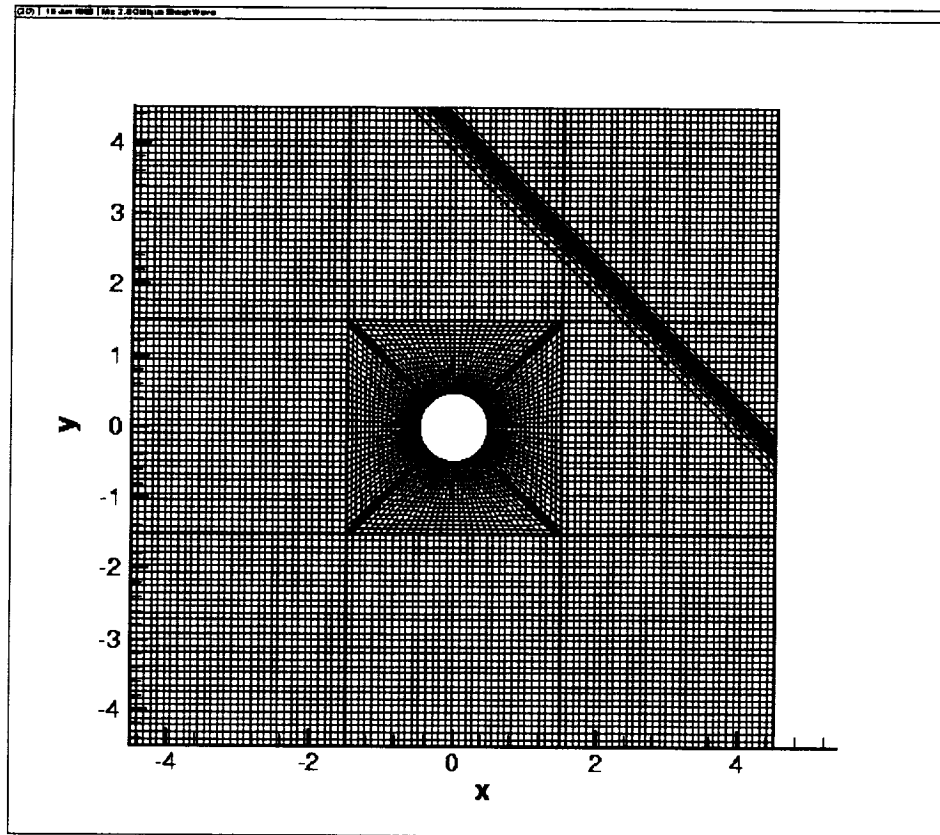[35] B. GUSTAFSSON, *The Convergence Rate for Difference Approximations to General Mixed Initial Bound-*

FIG. 6.10. *Propagating viscous shock.*

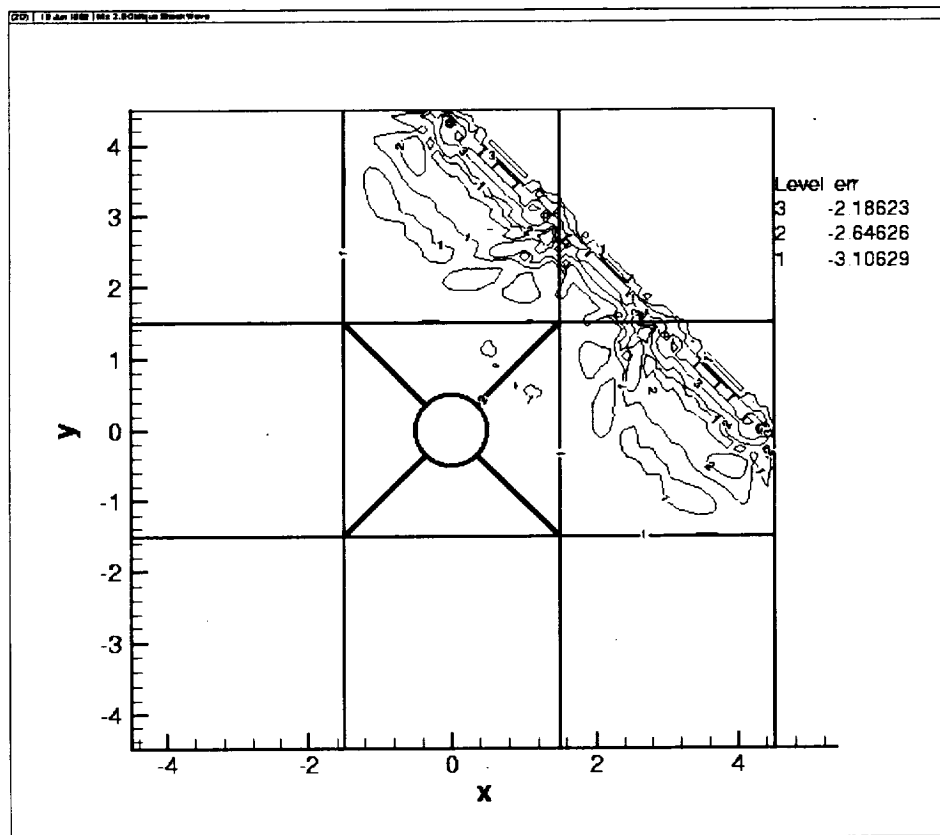*ary Value Problems*, SIAM J. Numer. Anal., 18, No. 2, (1981).

FIG. 6.11. *Local error levels for propagating viscous shock.*

REPORT DOCUMENTATION PAGE

Public reporting burden for this collection of information is estimated to average 1 hour per response, including the time for reviewing instructions, searching existing data sources, gathering and maintaining the data needed, and completing and reviewing the collection of information. Send comments regarding this burden estimate or any other aspect of this collection of information, including suggestions for reducing this burden, to Washington Headquarters Services, Directorate for Information Operations and Reports, 1215 Jefferson Davis Highway, Suite 1204, Arlington, VA 22202-4302, and to the Office of Management and Budget, Paperwork Reduction Project (0704-0188), Washington, DC 20503.

1. AGENCY USE ONLY*(Leave blank)*	2. REPORT DATE	3. REPORT TYPE AND DATES COVERED
	December 1999	Contractor Report

4. TITLE AND SUBTITLE

High order finite difference methods, multidimensional linear problems and curvilinear coordinates

5. FUNDING NUMBERS

C NAS1-97046
WU 505-90-52-01

6. AUTHOR(S)

Jan Nordström
Mark H. Carpenter

7. PERFORMING ORGANIZATION NAME(S) AND ADDRESS(ES)

Institute for Computer Applications in Science and Engineering
Mail Stop 132C, NASA Langley Research Center
Hampton, VA 23681-2199

8. PERFORMING ORGANIZATION REPORT NUMBER

ICASE Report No. 99-54

9. SPONSORING/MONITORING AGENCY NAME(S) AND ADDRESS(ES)

National Aeronautics and Space Administration
Langley Research Center
Hampton, VA 23681-2199

10. SPONSORING/MONITORING AGENCY REPORT NUMBER

NASA/CR-1999-209834
ICASE Report No. 99-54

11. SUPPLEMENTARY NOTES

Langley Technical Monitor: Dennis M. Bushnell
Final Report
To be submitted to the Journal of Computational Physics.

12a. DISTRIBUTION/AVAILABILITY STATEMENT

Unclassified–Unlimited
Subject Category 64
Distribution: Nonstandard
Availability: NASA-CASI (301) 621-0390

12b. DISTRIBUTION CODE

13. ABSTRACT *(Maximum 200 words)*

Boundary and interface conditions are derived for high order finite difference methods applied to multidimensional linear problems in curvilinear coordinates. The boundary and interface conditions lead to conservative schemes and strict and strong stability provided that certain metric conditions are met.

14. SUBJECT TERMS

high-order finite-difference, numerical stability, interface conditions, summation-by-parts, variable coefficient

15. NUMBER OF PAGES

35

16. PRICE CODE

A03

17. SECURITY CLASSIFICATION OF REPORT	18. SECURITY CLASSIFICATION OF THIS PAGE	19. SECURITY CLASSIFICATION OF ABSTRACT	20. LIMITATION OF ABSTRACT
Unclassified	Unclassified		